V 11 – 12. 4. 2021

1 On the cortical mapping function – visual space, cortical
2 space, and crowding

3 Hans Strasburger

4 Ludwig-Maximilians-Universität München

5 www.hans.strasburger.de

6 For submission to *Vision Research*

7 Abstract

8 The retino-cortical visual pathway is retinotopically organized: Neighbourhood relationships
9 on the retina are preserved in the mapping to the cortex. Size relationships in that mapping
10 are also highly regular: The size of a patch in the visual field that maps onto a cortical patch
11 of fixed size follows, along any radius and in a wide range, simply a linear function with
12 retinal eccentricity. As a consequence, and under simplifying assumptions, the mapping of
13 retinal to cortical locations follows a logarithmic function along that radius. While this has
14 already been shown by Fischer (1973), the link between the linear function – which
15 describes the local behaviour by the cortical magnification factor M – and the logarithmic
16 location function for the global behaviour, has never been made fully explicit. The present
17 paper provides such a link as a set of ready-to-use equations using Levi and Klein's E_2
18 nomenclature, and examples for their validity and applicability in the retinotopic mapping
19 literature are discussed. The equations allow estimating M in the retinotopic centre and
20 values thus derived from the literature are provided. A new structural parameter, d_2, is
21 proposed to characterize the cortical map, as a cortical counterpart to E_2, and typical values
22 for it are given. One pitfall is discussed and spelt out as a set of equations, namely the
23 common myth that a pure logarithmic function will give an adequate map: The popular
24 omission of a constant term renders the equations ill defined in, and around, the retinotopic
25 centre. The correct equations are finally extended to describe the cortical map of Bouma's
26 law on visual crowding. The result contradicts recent suggestions that critical crowding
27 distance corresponds to a constant cortical distance.

31 Introduction

32 One of the most beautiful organizational principles of the human brain is that of
33 topographical mapping. Whilst perhaps universal to the brain, its regularity is most apparent
34 for the three primary senses mediated through the thalamus – sight, hearing, and touch –
35 i.e., in retinotopy, tonotopy, and somatotopy. For the visual domain with which we are
36 concerned here, the regularity of topography is particularly striking and is at a level that
37 lends itself to mathematical description by analytic functions. The seminal papers by Fischer
38 (1973) and Schwartz (1977, 1980) derive the complex logarithm as a suitable function for
39 mapping the location in the visual field to the location of its projection's in (a flat-map of)
40 the primary visual cortex, by which the visual field's polar-coordinate grid gets mapped onto

41   a rectilinear cortical grid. The log function's image domain – the complex plane – is
42   reinterpreted thereby as a two-dimensional real plane.[1] As Schwartz explains in the two
43   papers, the rationale for employing the log function in the radial direction is that its first
44   derivative is an inverse-linear function, the latter implicit in the cortical magnification
45   concept for the visual field as proposed by Daniel & Whitteridge (1961). Expressed more
46   directly, the *integral* of an inverse linear function is the logarithmic function. Intuitively,
47   summing-up (integrating over) little steps on the cortical map, where each step obeys
48   cortical magnification, will result in the log mapping.

49   Schwartz's (1977, 1980) papers with the complex-log mapping have become rather popular
50   in visual psychophysics and visual neurophysiology. Van Essen, Newsome & Maunsell (1984),
51   e.g., use it for explaining the topography of the macaque's primary visual cortex, writing
52   "Along the axis corresponding to constant polar angle, magnification is inversely
53   proportional to eccentricity, and hence distance is proportional to the logarithm of
54   eccentricity (x $\propto$ log E)" (p. 437). Levi, Klein & Aitsebaomo (1985, Fig. 14) and Virsu et al.
55   (1987, Fig. 7) plot psychophysical thresholds in terms of cortical units. As another example,
56   Klein & Levi (1987), in the context of modelling hyperacuity in peripheral vision, derive from
57   the log rule that, if vernier-acuity offsets are assumed to have a constant cortical
58   representation – i.e. one that is independent of eccentricity – vernier offsets will depend
59   linearly on eccentricity in the visual field (we will come back to that in the last section).
60   Horton & Hoyt (1991) use it to point out that the well-known inverse-linear function for the
61   cortical magnification factor M (CMF) follows from a log-spaced cortical map. Engel et al.
62   (1997, Fig. 9, Fig 12; 1994, Fig. 2), and Larsson & Heeger (2006), use the (real-valued) log
63   function implicitly when they use an exponential for the inverse location function (which
64   corresponds to a log forward mapping). Duncan & Boynton (2003) fit their fMRI activity
65   maps for the V1 topology using Schwartz's complex-log mapping. The most advanced
66   development is Schira, Tyler, Spehar & Breakspear's (2010) closed-form analytic
67   representation for the cortical maps, at the same time accommodating for the horizontal-
68   vertical anisotropy and preserving cortical area constancy across meridians by an added
69   shear function.

70   While Fischer's and Schwartz's papers present the mathematical relationships
71   (withexamples for their application) Klein & Levi (1987) provide an *empirical* link between
72   psychophysical data and location on the cortical map. For characterizing the inverse-linear
73   CMF-vs-eccentricity function, they use a concept they had developed earlier for
74   psychophysical results (Levi, Klein, & Aitsebaomo, 1984; Levi et al., 1985): The slope of that
75   linear function, when normalized to the foveal value, can be quantified by a single number,
76   called E_2. The concept is illustrated graphically in Figure 1B below: In an x-y plot vs
77   eccentricity, E_2 is the (negative) X-axis intercept or, alternatively, the (positive) eccentricity
78   value at which the foveal value is incremented by itself (i.e., doubles). Klein & Levi (1987)
79   further bridge the gap to proportionality when they show that relationships become simpler
80   and more accurate when the data are not treated as a function of eccentricity E itself, but of
81   a transformed eccentricity, E^*, referred to as *effective eccentricity, $E^* = E + E_2$*. The *linear*
82   cortical magnification function thereby turns into *proportionality*. In the cortical map,
83   locations – i.e. distances from the retinotopic centre – are then proportional to the

---

[1] Note that the elegance of the complex-log representation is deceiving in that not all properties of the complex plane have a counterpart in the 2D real plane (which is undesirable for a mathematical represetnation). For example, the square of a value on the upper vertical meridian does not correspond to a value on the left horizontal meridian, as would be implied by $i^2 = -1$.

84   logarithm of effective eccentricity, x $\propto$ log *(E+E$_2$)*. The approach is verified by showing the
85   empirical data both as thresholds and in cortical units (Klein & Levi, 1987, Fig. 5; for rescaling
86   that figure's right ordinate the authors posit that 1 mm of cortex corresponds to ~10% of
87   effective eccentricity).

88   However, the papers discussed so far have not yet fully exploited the tight mathematical link
89   between the linear and the logarithmic law for its empirical use. While the basic
90   mathematical form of the mapping function $-$ log *(E) or* log *(E+E$_2$)* $-$ is drawn upon and made
91   use of, further parameters are left free to vary and to be determined by fitting to the data.
92   The derivations in the present paper take the log-mapping approach one step further. Unlike
93   these and other papers (discussed below), the parameters for the logarithmic map are here
94   obtained by mathematical derivation from the linear law. In a neuroscience context, that law
95   will be the inverse of the CMF. For the psychophysicist, measures of low-level visual-
96   perceptual function like the minimal angle of resolution (MAR) can be an approximation. In
97   both cases, Levi and Klein's E_2 concept is the basis here. We thereby arrive at a set of fully
98   explicit equations that allow converting the linear, local-behaviour law of the CMF, specified
99   by E_2, to a description of the global behaviour, the *location* on the cortical map. These
100   equations are the message of the paper. In a next step, the empirical data for the cortical
101   maps (from fMRI or single-cell analysis) are then used to verify the correctness of those
102   parametrical equations. This approach represents a more principled one than before. It
103   further places additional constraints on the describing functions, thus adding to their
104   reliability.

105   Since such derivations have been attempted before and have led to erroneous results or
106   have stopped short of exploring the implications, derivations are presented in a step-by-step
107   manner, considering at each step what that means. Key equations are highlighted by
108   surrounding boxes for easy spotting, i.e. those that should be of practical use in describing
109   the cortical map. Or, for example, for obtaining improved estimates for the foveal CMF, M_0.

110   Instead of the complex log we here consider the simpler case of the real-valued, 1D
111   mapping, where *eccentricity* in the visual field, expressed in degrees of visual angle along a
112   radius, is mapped onto the *distance* of its representation from the retinotopic centre,
113   expressed in millimetres. The resulting real-valued logarithmic function shall be called the
114   *cortical location function*. Taking the 1D case implies no loss of generality; the function is
115   easily generalized to the 2D case by writing it as a vector function. Compared to the complex
116   log, the real function has the added advantage of allowing separate parameters for the
117   horizontal and vertical meridian, required to meet the visual field's horizontal-vertical
118   anisotropy.

119   Once these relationships for the cortical location function are established, they need to be
120   verified by empirical data. We use data from the literature and our own for this. It turns out
121   that not only do the fits work excellently, and even better than the original fits, but that the
122   constraints imposed by the parametric equations can also be used for the long-standing
123   problem of improving estimates for the foveal CMF (M_0). Another issue addressed there are
124   attempts to become independent of the retinotopic centre's location. That centre's exact
125   location appears to be difficult to find (it is often specified only approximately), and some
126   authors like to use some other reference location instead. It turns out, however, that while
127   equations can be referenced to some other location than the centre, true independence
128   from the latter cannot be achieved by any means.

3

129 In the context of these derivations, I propose a new metric, d_2, measured in millimetres, for
130 characterizing the cortical map. It is the equivalent of E_2 (which is measured in degrees visual
131 angle). Like E_2 in the visual field, d_2 allows specifying the steepness of location change in the
132 cortical map, e.g. for quantifying the horizontal-vertical anisotropy or even for comparisons
133 between species.

134 In another section, it is further argued that the simplified version ($x \propto \log E$) that is not
135 uncommon in the fMRI literature needs to be avoided and that the full version with a
136 constant term added in *the log's argument* needs to be employed (i.e., $x \propto \log (E + c)$). There
137 is further apparently confusion about what does and what does not represent the required
138 constant term, which adds to a common myth that omitting the term simplifies matters.

139 Finally, the cortical location function can be used, perhaps unexpectedly, to derive the
140 cortical distances in visual crowding. Crowding happens when neighbouring patterns to a
141 target stimulus are closer than a critical distance; that critical distance can be described by
142 Bouma's law (Bouma, 1970; Strasburger, Harvey, & Rentschler, 1991; Pelli, Palomares, &
143 Majaj, 2004; Pelli & Tillman, 2008; Whitney & Levi, 2011; Strasburger, 2020). We thus arrive
144 at a cortical version of Bouma's law. While this has been done before (Levi et al., 1985;
145 Motter & Simoni, 2007; Pelli, 2008; Nandy & Tjan, 2012; Strasburger, Rentschler, & Jüttner,
146 2011; Strasburger & Malania, 2013), the present derivations go beyond those in that they
147 include the fovea and provide the derivations.

1. Concepts

149 Peripheral vision is unlike central vision as Ptolemy (90–168) already noted. Yet just how it is
150 different is still a puzzling question. The goal here is to draw the attention to the highly
151 systematic organization of the early neural processing stages by deriving equations that
152 describe its architecture. But before doing so we need to be explicit on a number of
153 concepts that are the foundation for what follows.

154 *The linear law and the hyperbola graph.* Four types of analytic functions are central for
155 describing functional dependencies on eccentricity – in the visual field or in retinotopic
156 areas: linear and inverse-linear, and logarithmic and exponential. Their graphs look entirely
157 different (giving rise to misleading intuition; Rosenholtz, 2016, Strasburger, 2020) yet the
158 first two and second two are effectively equivalent to each other. Let's start with the first
159 pair (the second pair follows in Figure 3).

160 Aubert and Foerster's (1857) characterization of the performance decline with retinal
161 eccentricity as a linear increase of minimum resolvable size – sometimes referred to as the
162 Aubert-Foerster law – is still the conceptual standard. It corresponds to what is now called
163 *M-scaling* when based on cortical magnification (Virsu & Rovamo, 1979; Virsu et al., 1987) or
164 the change of *local spatial scale* when the scaling factor is not thus constrained (Watson,
165 1987). Examples for the linear law are shown in Figure 1A and 2A. However, by the end of
166 the 19th century it also became popular to use the inverse of minimum size instead, i.e.
167 acuity, in an attempt to make the sensory decline more graphic (e.g. Fick, 1898, shown in
168 Figure 1B). And, since the inverse-linear function's graph is close to a hyperbola, we arrive at
169 the well-known hyperbola-like function of, e.g., acuity vs. eccentricity seen in most
170 textbooks, or in Østerberg's (1935) equally well-known cone-density graph. Examples of that
171 graph for the cortical map are in Dougherty et al. (2003, Fig. 5) and Harvey & Dumoulin
172 (2011, Fig. 4B), shown in Figure 1 C and D.

A
$$y = aE + b$$

B
$$y = \frac{1}{aE + b}$$

C
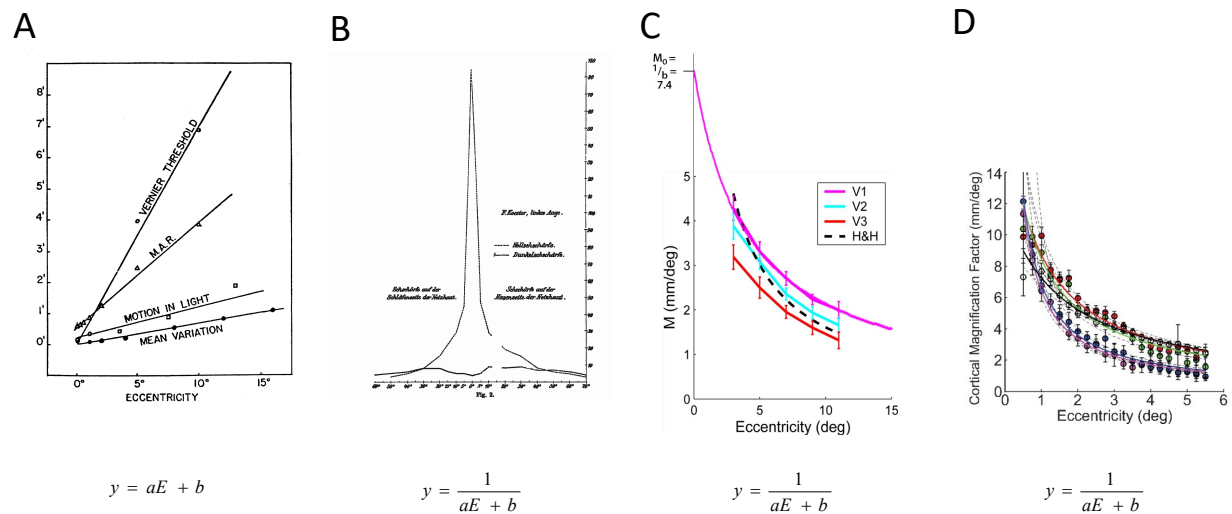$$y = \frac{1}{aE + b}$$

D
$$y = \frac{1}{aE + b}$$

Figure 1. Examples for the linear and the inverse-linear (approx. hyperbola) graph. Even though the two are equivalent, their intuitive interpretation is often different, with the linear graph taken as evidence of a shallow performance decline and the inverse-linear graph as evidence of a steep decline (Rosenholtz, 2016; Strasburger 2020). A. MAR for various visual performance parameters; Weymouth (1958, Fig. 13). B. Visual acuity; Fick (1898, Fig. 2). C. Cortical magnification factor *M*; Dougherty et al. (2003, Fig. 5). A hyperbola graph, obtained from linear regression to the inverse data ($M=1/(0.033E+0.1355)$), and an axis intercept $M_0=1/b$ have been added to the original graph. D. Same; Harvey & Dumoulin, 2011, Fig. 4B. In C and D note the steep incline toward the retinotopic centre and that no data are obtained in or near the centre. The central value M_0 is therefore difficult to derive directly from those graphs.

173   Yet, graphic as it may be, the hyperbola graph does not lend itself to a comparison of decline
174   parameters. Weymouth (1958) therefore already argued for using the linear graph,
175   introducing the concept of the *minimal angle of resolution* (MAR) as a general measure of
176   size threshold. Weymouth summarized how the MAR and other spatial visual performance
177   parameters depend on retinal eccentricity (Figure 1A). Importantly, Weymouth stressed the
178   *mandatory use* of a non-zero, *positive y-axis intercept* for these functions (Weymouth, 1958,
179   p. 109). This will be a major point here in the paper; it is related to the necessity of a
180   constant term in the cortical-location function as discussed below.

181   *Cortical magnification.* Daniel & Whitteridge (1961) and Cowey & Rolls (1974) introduced
182   cortical magnification as a quantitative concept for retinotopic mapping, which, for a given
183   visual-field location, summarizes functional density along the retino-cortical pathway into a
184   single number. The linear cortical magnification factor (CMF), *M,* was defined as the
185   *diameter in the primary visual cortex onto which 1 deg of the visual field projects* (*areal M*
186   was defined as an areal counterpart). Enlarging peripherally presented stimuli by *M* turns
187   out to counter performance decline to a large degree for many visual tasks (reviewed, e.g.,
188   by Virsu et al., 1987); it was thus suggested as a general means of equalizing visual
189   performance across the visual field (Rovamo & Virsu, 1979). Even though this so-called
190   strong hypothesis was soon dismissed (e.g. Westheimer, 1982, p. 161), the strong tie
191   between cortical distances and (in particular) low-level psychophysical tasks is still striking.

192   The relationship between the early visual architecture and psychophysical tasks is still a
193   matter of debate; why, for example, do different visual tasks show widely differing slopes of
194   their eccentricity functions (Figure 1A)? In contrast, the manner in which the CMF varies
195   with eccentricity is largely agreed upon: *M* decreases with eccentricity – following

196   approximately a hyperbola (Figure 1C and D) – and its inverse increases linearly (Schwartz,
197   1980; Van Essen et al., 1984; Tolhurst & Ling, 1988; Horton & Hoyt, 1991, Slotnick, Klein,
198   Carney, & Sutter, 2001, Duncan & Boynton, 2003; Larsson & Heeger, 2006; Schira, Wade, &
199   Tyler, 2007). Figure 2A shows a few examples for the latter. Note that in the figure there is
200   one function from psychophysics shown along with the anatomical estimates (Rovamo &
201   Virsu, 1979; Virsu & Rovamo, 1979; Virsu et al., 1987). Note also that all functions need to
202   have a positive y-axis intercept, *be it ever so slight,* because otherwise *M* were undefined,
203   i.e., infinite.

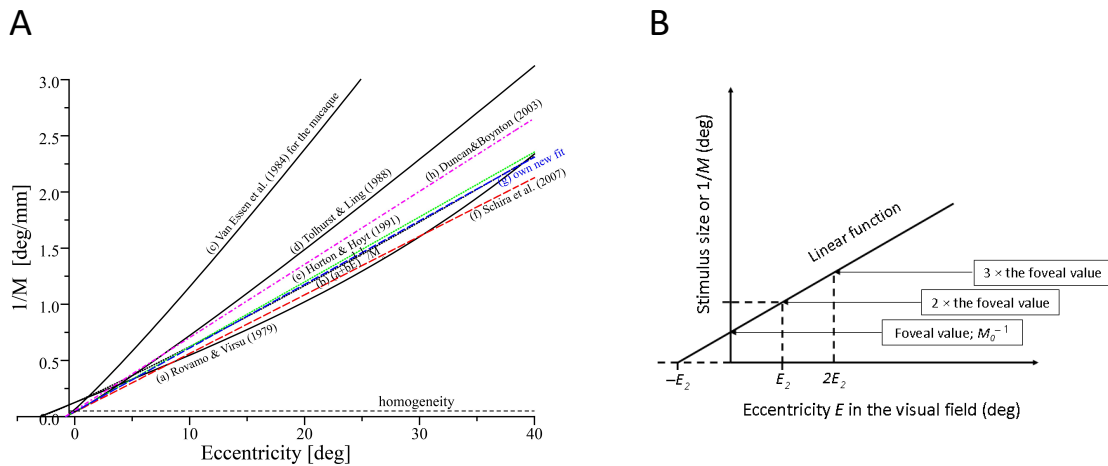A   B

Figure 2. A. The inverse of the cortical magnification factor or, equivalently, the size of a patch in the visual field that projects onto a patch of constant size in the cortex, as a function of eccentricity in the visual field (Fig. 9 in Strasburger et al., 2011, reproduced for illustrating the text). All functions show a mostly linear behaviour. Their slope is quite similar, with the exception of Van Essen et al.'s (1984) data for the macaque; other data show similar slopes between human and monkey (e.g. Oehler, 1985). Note that Rovamo & Virsu's function is based on psychophysical data. Note also that all functions need to have a positive y-axis intercept. B. An illustration of the E_2 concept. E_2 is defined as the eccentricity where the foveal value doubles, or (equivalently) as the eccentricity increment that leads to an increment by the foveal value. It is also the negative x-axis intercept. Note that the foveal value does not double *every E_2* increment (cf. Strasburger, 2020). Importntly, note that the concept can be used for both psychophysical and anatomical data.

204   *Other equations:* Empirical data typically fit the linear concept quite well in the considered
205   range of about 40° eccentricity, but, nevertheless, fits can sometimes be improved by
206   introducing a slight nonlinearity (Table 1). Rovamo, Virsu, & Näsänen (1978), as an example,
207   used a polynomial by adding a small 3rd-order term; Van Essen et al. (1984), Tolhurst & Ling
208   (1988), and Sereno et al. (1995) increased the exponent of the linear term slightly above 1.
209   Virsu & Hari (1996) used a sine function, based on geometrical considerations. Only a part of
210   the sine's period comes into play so that the function is still close to linear in that range. The
211   latter function is interesting because it is the only one that can be extended to eccentricities
212   larger than 90°(cf. Strasburger, 2020). However, improvements over a linear approach are
213   mostly small or absent and do not warrant the added complexity in the derivations to follow,
214   so we will not pursue this further.

6

Equation	Source	Comments
$M^{-1} = M_0^{-1} \cdot (1 + aE)$	Cowey & Rolls (1974) (data from Wertheim, 1894) Schira et al., 2010 Harvey & Dumoulin, 2011	Inverse-linear equation
$M^{-1} = M_0^{-1} \cdot (1 + E/E_2)$	Levi et al. (1985, Table 1) Klein & Levi (1987) Horton & Hoyt (1991) Dougherty et al. (2003)	Inverse-linear equation using E_2.
$M^{-1} = M_0^{-1} \cdot (1 + aE + bE^3)$	Rovamo & Virsu (1979)	Nonlinearity by an added small 3rd-order term
$M^{-1} = M_0^{-1} \cdot (1 + aE)^\alpha$	Van Essen et al. (1984), $\alpha=1.1$ Tolhurst & Ling (1988) , $\alpha=1.1$ Sereno et al (1995), $\alpha=1.26$	Non-linearity by an added exponent α close to 1
$M^{-1} = a + b \sin(E)$	Virsu & Hari (1996), Näsänen & O'Leary (2001)	Only $^1/_8$ of the sine period is used

215   Table 1. Equations used for describing eccentricity functions (modified from Strasburger et al., 2011).

216   *The E_2 concept.* For a quick comparison of eccentricity functions, Levi et al. (1984, p. 794)
217   introduced the E_2 concept by pointing out the specific eccentricity at which the respective
218   foveal value doubles (Figure 2B). More generally, E_2 is the *eccentricity increment* at which y
219   increases by the foveal value. I.e., at eccentricity E_2 the foveal value is doubled and at twice
220   E_2 is tripled. As a graphic aide, E_2 is also the distance from the origin of where the linear
221   function crosses the eccentricity axis.

222   E_2 is most often used for psychophysical tasks but lends itself equally well for describing the
223   anatomical function (Levi et al., 1985, Table 1; Klein & Levi, 1987; Horton & Hoyt, 1991;
224   Dougherty et al., 2003). Eq. (1) states the corresponding equation.

225    $M^{-1}/M_0^{-1} = E/E_2 + 1$.   (1)

226   M^{-1} in that equation is measured in °/mm (one might call it the retinal magnification factor:
227   it corresponds to the receptive field size of a cortical neuron on the retina). M_0^{-1} is that value
228   in the fovea's centre. The function's slope is given by M_0^{-1}/E_2, so when these functions are
229   normalized to the foveal value, their slope is $1/E_2$. I.e., larger E_2 corresponds to shallower
230   slope. Parameter E_2 thus captures an important property of the functions (how they
231   increase/decrease) in a single number. A summary of values was reported by Levi et al.
232   (1984), Levi et al. (1985), Klein & Levi (1987), or more recently by Strasburger et al. (2011,
233   Tables 4–6). These reported E_2 values vary widely between different visual functions. They
234   also vary considerably for functions that seem directly comparable to each other (for
235   example, E_2 for vernier acuity: 0.62°–0.8°; for M^{-1}: 0.77°–0.82° or even 3.67° in Dougherty et
236   al., 2003; for Landolt-C acuity: 1.0°–2.6°; letter acuity: 2.3°–3.3°; gratings: 2.5°–3.0°). On the
237   other hand, E_2 can also be surprisingly similar for tasks that seem entirely unrelated, like for
238   example the E_2 of 1.22° for the perceived travel extent in the fine-grain movement illusion
239   (Foster, Thorson, McIlwain, & Biederman-Thorson, 1981). Note also the limitations of E_2:
240   since, for example, the empirical functions always deviate a little from linearity, the
241   characterization by E_2, by its definition, works best at small eccentricities.

242   *M-scaling and local scale:* The left hand ratio in eq. (1), M^{-1}/M_0^{-1}, is the ratio by which a
243   peripherally seen stimulus needs to be size-scaled to occupy cortical space equal to a foveal
244   stimulus. So the equation can be re-written as

245 $$S/S_0 = E/E_2 + 1,$$ (2)

246   where S is *scaled size* and S_0 is the size at the fovea's centre. S_0 can be considered the size-
247   scaling unit in the visual field, and E_2 the locational scaling unit (i.e. the unit in which scaled
248   eccentricities are measured). If E_2 refers to the cortical map, this is the *concept of M-scaling*.
249   If E_2 in the equation refers to some other eccentricity function, this corresponds to a more
250   abstract way of size scaling, called *local scale* (Watson, 1987).

251   *The cortical location function:* Fischer (1973) and Schwartz (1977, 1980) proposed the
252   complex log function for mapping the visual field to the cortical area. The key property of
253   interest for that mapping is the behaviour *along a radius* (from the fovea) in the visual field;
254   the simpler real-valued log function can thus be used instead of the complex logarithm. This,
255   then, maps the eccentricity in the visual field to the distance from the retinotopic centre on
256   the cortical map (Figure 3B). Neuroscience papers often prefer to show the inverse function
257   (i.e. mirrored along the diagonal with the x and y axis interchanged, thus going "backwards"
258   from cortical distance to eccentricity), which is the exponential function shown schematically
259   in Figure 3A.

260   *The constant term:* Schwartz (1980) has discussed two versions of the function that differ in
261   whether there is a constant term added in the argument; the difference is illustrated in the
262   graph. The version without the constant is often considered simpler and is thus often
263   (inappropriately) preferred. A point in the following will be that that simplicity is deceiving
264   and can lead to wrong conclusions – and more complicated equations. Note that the
265   constant term is at different places in the equations: For the exponential function in figure
266   part (A) it is *added to* the exponential, for the logarithmic function in (B) it is *within* the log's
267   argument. As will be seen later, the constant term in both cases corresponds to the positive
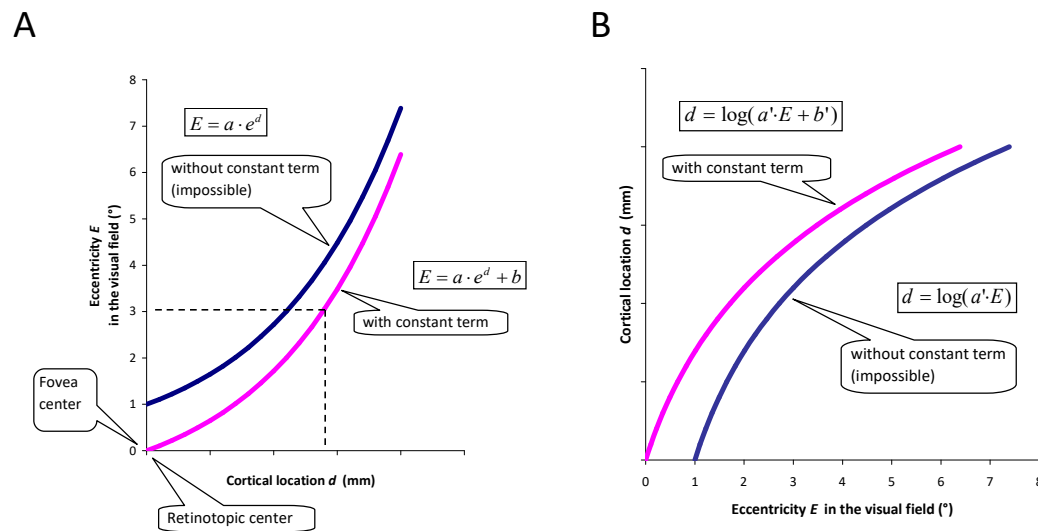268   y-intercept of the linear function (Figure 2B).

8

Figure 3. Schematic graph of the cortical location function introduced by Fischer (1973) and Schwartz (1977, 1980), along a radius from the retinotopic centre. A version with, and another without a constant term (parameter *b* or *b'* in the equation) are shown. The constant term's omission was intended as a simplification for large eccentricities but is not physically possible near or in the foveal centre. The graph in (A) shows eccentricity *E* as a function of cortical distance *d* (which is an exponential); Schwartz (1980) discussed mainly the inverse function shown in (B), i.e. for *d* as a function of *E* (which is logarithmic).

269 *The retinal and the retinotopic centre:* There is an important difference in difficulty between
270 measuring at the fovea's exact centre and at the cortical retinotopic counterpart. Whereas
271 psychophysical measurements at the fovea are particularly simple and reliable, determining
272 the exact retinotopic centre and the CMF at that location, M_0, appear the most difficult and
273 M_0's value is mostly extrapolated from peripheral values. The consequences of this include
274 different strategies in research between the two fields regarding the map.

275 *Anisotropy.* The visual field is not isotropic: Performance declines differently between radii.
276 Slopes differ between vertical and horizontal, and upper vs lower field. Accordingly, iso-
277 performance lines (for the binocular field) are distorted ellipses rather than circular outside
278 the central visual field, which is isotropic (e.g. Wertheim, 1894, Harvey & Pöppel, 1972;
279 Pöppel & Harvey, 1973). Rovamo & Virsu (1979, p. 498) accordingly computed separate *M*
280 estimates for each meridian. There is further a nonlinearity at the transition from the
281 isotropic to the anisotropic field (Pöppel & Harvey, 1973, Fig. 6). Correspondingly, early
282 visual areas are also anisotropic (e.g. Horton & Hoyt, 1991). The effect of anisotropy on the
283 cortical magnification factor is quantitatively treated by Schira et al. (2007, 2010); their M_0
284 estimate is the geometric mean of the isopolar and isoeccentric *M* estimates. In the
285 equations presented below, the horizontal/vertical anisotropy can be accommodated by
286 letting the parameters depend on the radius in question. There are further anisotropies that
287 are not accounted for by varying slopes along the radii (Schira et al., 2007, 2010). These
288 authors, for preserving *area* constancy across meridians, thus extend modelling by a shear
289 function (using the hyperbolic secans; Schira et al., 2010, eq. 6 and Fig. 2). Mappings then
290 differ between meridians, with deviations from linearity most noticeable on, and close to,
291 the vertical meridian at around 1° eccentricity (Schira et al., 2010, Fig. 2). The derivations
292 presented below, for simplicity, do not include these refinements.

293 *Symbols in the paper:* To keep the overview, symbols used in the paper are summarized in
294 Table 2. Some of those are in standard use and some are newly introduced in the remainder.

9

295

	Visual Field	Cortical Map
Cortical magnification factor	M^{-1}	M
Stimulus size	S	–
Location as distance from the centre	E	d
Location as distance from a reference	–	$\hat{d}$
Levi and Klein's E_2	E_2	d_2
Location of reference as distance from the centre	–	d_{ref}
Critical distance for crowding	δ	κ
Critical distance for crowding in the very centre	δ_0	κ_0
E_2 for critical crowding distance	$\hat{E}_2$	–

296   Table 2. Summary of symbols used in the paper

2. The cortical location function

2.1 Cortical location specified relative to the retinotopic centre

299   The ratio S/S_0 in eq. (2) is readily estimated in psychophysical experiments as the size of a
300   stimulus relative to its foveal value for achieving equal perceptual performance. However, its
301   physiological counterpart M^{-1}/M_0^{-1} in eq. (1) appears difficult to assess directly, even though
302   it is a physiological concept. Instead, it is typically derived by extrapolation from peripheral
303   values, e.g. from the cortical-location function $d = d(E)$ (Figure 3). The function links a cortical
304   distance d in a retinotopic area to the corresponding distance in the visual field that it
305   represents. More specifically, d is the distance (in mm) on the cortical surface between the
306   representation of a visual-field point at eccentricity E, and the representation of the fovea
307   centre. Under the assumption of linearity of the cortical magnification function $M^{-1}(E)$, this
308   function is logarithmic (Figure 3B) and its inverse $E = E(d)$ exponential (Figure 3A), as shown
309   by Fischer (1973) and Schwartz (1977, 1980). Since the E_2 parameter allows a simple
310   formulation of the linear eccentricity functions (Figure 2), as e.g. in eq. (1), it will be useful to
311   state the location function with those notations. First steps have been derived in Strasburger
312   et. al. (2011, eqs. 10 – 13; corresponding here eqs. 3 – 6). The present derivations go further.
313   The location function allows a concise quantitative characterization of the early retinotopic
314   maps.

315   For its derivation, notice first that, locally, the cortical distance of the respective
316   representations $d(E)$ and $d(E+\Delta E)$ of two nearby points along a radius, at eccentricities E and
317     $E+\Delta E$, is given by $M(E)\cdot\Delta E$. This follows from M's definition and the fact that M refers to 1°.
318   The cortical magnification factor M is thus the first derivative of $d(E)$, i.e.,

319     $$M = d'(E).$$ (3)

320   Conversely, the location d on the cortical surface (i.e., the global aspect) is the integral over
321   M, starting at the fovea centre:

322     $$d(E) = \int_0^E M(E)dE.$$ (4)

323   If we insert eq. (1) – i.e. the equation using E_2 – into eq. (4), we have

10

324 $$d(E) = \int_0^E \frac{M_0}{1 + E/E_2} dE$$

325 $$= M_0 E_2 \ln(1 + E/E_2) \text{ (with } E \geq 0\text{)},$$ (5)

326 where ln denotes the natural logarithm.

327 The inverse function, $E(d)$ is derived by inverting eq. (5),

328 $$E = E_2(e^{\frac{d}{M_0 E_2}} - 1) \text{ (with } d \geq 0\text{)}.$$ (6)

329 It states how the eccentricity E in the visual field depends on the distance d of the
330 corresponding location in a retinotopic area from the retinotopic centre. With slight
331 variations, discussed below, it is the formulation often referenced in fMRI papers on the
332 cortical mapping. Note that, by its nature, it is only meaningful for positive values of cortical
333 distance d. The significance of this point will become apparent later.

334 We can simplify that function further by introducing an analogue to E_2 in the cortex. Observe
335 that like any point in the visual field the location at E_2 has a representation (on the meridian
336 in question), whose distance from the retinotopic centre we denote as d_2. Thus, d_2 in the
337 cortex represents E_2 in the visual field.

338 To express eq. (6) using d_2 instead of M_0, first apply the equation to that location d_2:

339 $$E_2 = E_2(e^{\frac{d_2}{M_0 E_2}} - 1) \ .$$ (7)

340 Solving that for the product $M_0 E_2$ gives

341 $$M_0 E_2 = d_2 / \ln 2,$$ (8)

342 which, inserted into eq. (6) in turn gives

343 $$\boxed{E = E_2(2^{d/d_2} - 1)}.$$ (9)

344 Eq. (9) is the most concise way of stating the cortical location function. We can also restate it
345 however as

346 $$\boxed{E = E_2(e^{(\ln 2)d/d_2} - 1)}$$ (10)

347 since the exponential to the base e is often more convenient (ln again denotes the natural
348 logarithm).

349 This equation (eq. 10) is particularly nice and simple provided that d_2, the cortical equivalent
350 of E_2, is known. That value, d_2, could thus play a key role in characterizing the cortical map,
351 similar to the role of E_2 in visual psychophysics (cf. Table 4 – Table 6 in Strasburger et al.,
352 2011, or earlier the tables in Levi et al., 1984, Levi et al., 1985, or Klein & Levi, 1987).
353 Estimates for d_2 derived from literature data are summarized in Section 2.4 below, as an aid
354 for concisely formulating the cortical location function.

355 The new cortical parameter d_2 can be calculated from eq. (8), restated here for convenience:

356 $$\boxed{d_2 = M_0 E_2 \ln 2}$$ (8a)

11

2.2 Cortical location specified relative to a reference location

Implicit in the definition of d or d_2 is the knowledge about the location of the fovea centre's cortical representation, i.e. of the retinotopic centre. That locus has proven to be hard to determine precisely, However, and instead of the centre it has thus become customary to use some fixed eccentricity E_{ref} as a reference. Engel et al. (1997, Fig. 9; 1994, Fig. 2), for example, use E_{ref} = 10°. Larsson & Heeger (2006, Fig. 5) use E_{ref} = 3°.

To restate eq. (6) or (10) accordingly, i.e. with some reference eccentricity different from E_{ref} = 0, we first apply eq. (10) to that reference:

$$E_{ref} = E_2(e^{(\ln 2)d_{ref}/d_2} - 1),$$ (11)

where d_{ref} denotes the value of d at the chosen reference eccentricity, e.g. at 3° or 10°.

Solving then that equation for d_2 and plugging the result into eq. (9) or (10), we arrive at

$$E = E_2((E_{ref}/E_2 + 1)^{d/d_{ref}} - 1).$$ (12)

Expressed to the base e instead, we have

$$\boxed{E = E_2(e^{\beta(d/d_{ref})} - 1), \text{ with } \beta = \ln(\frac{E_{ref}}{E_2} + 1) \text{ (and } d \geq 0),}$$ (13)

which represents the location function expressed *relative to a reference eccentricity* E_{ref}, and its equivalent in the cortical map, d_{ref}. (One could also derive eq. (13) directly from eq. (6).) Note that if, in that equation, E_2 is taken as the reference eccentricity for checking, it reduces to eq. (10) as expected. So, E_2 can be considered as a special case of a reference eccentricity. Note further that, unlike the location equations often used in the retinotopy literature (Van Essen et al., 1984, in the introduction; Duncan & Boynton, 2003; Larsson & Heeger, 2006), the equations are well defined in the fovea centre: for d = 0, the eccentricity E is zero, as it should.

What reference to choose is up to the experimenter. However, the fovea centre itself cannot be used as a reference eccentricity – the equation is undefined for d_{ref} = 0 (since the exponent is then infinite). Thus, the desired independence of knowing the retinotopic centre's location has not been achieved – that knowledge is still needed, since d, and d_{ref}, in these equations are defined as the respective distances from that point.

Equations (12) and (13) have the ratio d/d_{ref} in the exponent. It is a proportionality factor for cortical distance. From the intercept theorem in geometry we know that this factor cannot be re-expressed by any other expression that leaves the zero point undefined. True independence from knowing the retinotopic centre, though desirable, thus cannot be achieved.

We can nevertheless shift the coordinate system such that locations are specified relative to the reference location, d_{ref}. For this, we define a new variable $\hat{d}$ as the cortical distance (in mm) from the reference d_{ref} instead of from the retinotopic centre (see Figure 4 for an illustration for the shift and the involved parameters), where d_{ref} is the location corresponding to some eccentricity, E_{ref}. By definition, then,
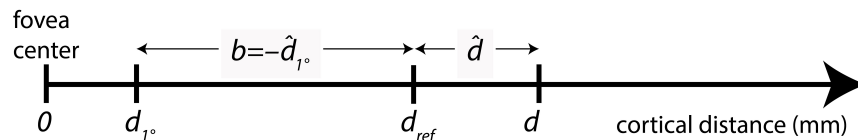
$$\hat{d} = d - d_{ref}$$ (14)

Figure 4: Illustration of the cortical distance measures used in equations (6) – (23), and of parameter b in eq. (18) further below.
d – cortical distance of some location from the retinotopic centre, in mm;
d_{ref} – distance (from the centre) of the reference that corresponds to E_{ref};
$d_{1°}$ – distance of the location that corresponds to $E = 1°$;
$\hat{d}$ – distance of location d from the reference d_{ref}.

396 In the shifted system – i.e., with $\hat{d}$ instead of d as the independent variable – eq. (6) for
397 example becomes

$$E = E_2 (e^{\frac{\hat{d} + d_{ref}}{M_0 E_2}} - 1).\tag{15}$$

399 The equation might be of limited practical use, however (like eq. 6 from which it was
400 derived), since the parameters M_0 and E_2 in it are not independent; they are inversely
401 related to each other as seen in eq. (8) or (8a) (or eq. 17). That interdependency is removed
402 in eq. (9) or (10), (which work from the retinotopic centre), or eq. (13) (which used a
403 reference eccentricity). The latter (eq. 13), in the shifted system becomes

$$\boxed{E = E_2 (e^{\beta \frac{\hat{d} + d_{ref}}{d_{ref}}} - 1)\text{, with } \beta = \ln(\frac{E_{ref}}{E_2} + 1) \text{ (and } \hat{d} + d_{ref} \geq 0).}\tag{16}$$

405 That equation now has the advantage over eq. (15) of having only two free parameters, E_2
406 and d_{ref}. (E_{ref} is not truly free since it is empirically linked to d_{ref}.) The foveal magnification
407 factor M_0 has dropped from the equation. Indeed, by comparing eq. (13) to eq. (6) (or by
408 comparing eq. (15) to (16)), M_0 can be calculated from d_{ref} and E_2 as

$$\boxed{M_0 = \frac{d_{ref}}{\beta \cdot E_2}},\tag{17}$$

410 where β is defined as in the previous equation. With an approximate location of the
411 retinotopic centre (needed for calculating d_{ref}) and an estimate of E_2, that latter equation
412 leads to an estimate of the foveal magnification factor, M_0 (see Section 2.4 for examples).

413 Equations (16) and (17) are crucial to determining the retinotopic map in early areas. They
414 should work well for areas V1 to V4 as discussed below. The connection between the linear
415 and log or exponential function based estimations provided by these equations allows cross-
416 validating the empirically found parameters and thus leads to more reliable results. Duncan
417 & Boynton (2003), for example, review the linear law and also determine the cortical
418 location function empirically but do not draw the connection. Their's and others' approaches
419 are discussed as practical examples in the section after next (Section 2.4).

2.3 Independence from the retinotopic centre with the simplified function?

421 Schwartz (1980) had offered a simplified location function where the constant term is
422 omitted, which works at sufficiently large eccentricities. Frequently that was the preferred

13

423   one by other authors as seemingly being more practical. The present section briefly
424   highlights how this approach leads astray if pursued rigorously.

425   The simplified version of the location function $E(\hat{d})$ omits the constant term in eq. (6) and
426   those that follow from it (i.e., the "−1" in eq. 6 up to eq. 16). Instead, the equation

427    $$E = e^{a(\hat{d}+b)} \tag{18}$$

428   is fit to the empirical data, with free parameters a and b. The distance variable in it is $\hat{d}$ as
429   before, i.e., the cortical distance from a reference d_{ref} representing some eccentricity E_{ref} in
430   the visual field. Engel et al. (1997, Fig. 9; 1994, Fig. 2), for example, use E_{ref} = 10° for such a
431   reference, and for that condition report the equation E = exp (0.063 ($\hat{d}$ + 36.54)). Larsson &
432   Heeger (2006, Fig. 5), as another example, use E_{ref} = 3°, and for area V1 in that figure give the
433   function E = exp (0.0577 ($\hat{d}$ + 18.0)). Note that neither of these equations contains the
434   required constant term (cf. Figure 3), since the constants (36.54 and 18.0) are inside, not
435   outside the exponential's argument.

436   We can attach meaning to the parameters a and b in eq. (18) by constraining the function
437   appropriately (see Strasburger, 2019, for the derivation). By that we arrive at an equation

438    $$E = E_{ref} \cdot (E_{ref}^{-\hat{d}/\hat{d}_{1°}}), \tag{19}$$

439   where $\hat{d}_{1°}$ is the distance of the 1° line from the reference eccentricity's representation; it is
440   around −36.5 mm for E_{ref} = 10° as used by Engel et al. (1994, 1997).

441   This is now the *simplified* cortical location function, i.e. the simplified analogue to eq. (16),
442   with parameters spelt out. One can easily verify that the equation holds true at the two
443   defining points, i.e. at 1° and the reference eccentricity. Note also that, as intended, knowing
444   the retinotopic centre's location in the cortex is not required since $\hat{d}$ is defined relative to a
445   non-zero reference. However, in between these two points the function has the wrong
446   curvature (see Fig. 4 in the next section, fat black line). Importantly, however, the equation
447   fails with small eccentricities, for the simple reason that E cannot become zero in that
448   equation. In other words, the fovea's centre is never reached, even at the retinotopic centre.

449   So the seeming simplicity of eq. (18) that we started out from leads astray in and around the
450   fovea – which, after all, is of prime importance for vision. The next section illustrates the
451   impact of the constant term with data from the literature.

452   **2.4 Practical use of the equations: examples**

453   **2.4.1 The approach of Larsson & Heeger (2006)**

454   Now that we have derived two sets of equations for the location function (i.e. with, and
455   without, a constant term in Section 2.1 and 2.3, respectively) let us illustrate the difference
456   with data on the cortical map. The first example are data from Larsson & Heeger (2006,
457   Fig. 5) for area V1. As a reminder, this is about eq. (16) on the one hand – in
458   essence $E = a(e^{b\hat{d}} - 1)$, derived from eq. (6) – and the discouraged eq. (18) or (19) on the
459   other hand (in essence $E = ae^{b\hat{d}}$, i.e. no constant term outside the exponent – Larsson &
460   Heeger's constant *'18.0' within* the exponent is part of the coefficient a).

461   For the reasons explained above, the retinotopic centre is left undefined by Larsson &
462   Heeger (2006), and a reference eccentricity of E_{ref} = 3° is used instead. The fitted equation in
463   the original graph in their paper is stated as E = exp (0.0577 ($\hat{d}$+18.0)), which corresponds to

464   eq. (18) with constants a = 0.0577, and $b = -\hat{d}_{1°}$ = 18.0. Its graph is shown in Figure 5 as the
465   thick black line copied from the original graph. It is continued to the left as a dotted blue line
466   to show the behaviour toward the retinotopic centre. At the value of $\hat{d} = -b$, i.e. at a distance
467   of $\hat{d}_{1°}$ = –18.0 mm from the 3° representation (as seen from eq. 18 or 19), the line crosses the
468   1° point. To the left of that point, i.e. towards the retinotopic centre, the curve deviates
469   markedly upward and so the retinotopic centre (E = 0°) is never reached.

Comparison of Laws, ref. Larsson & Heeger Fig. 5, V1
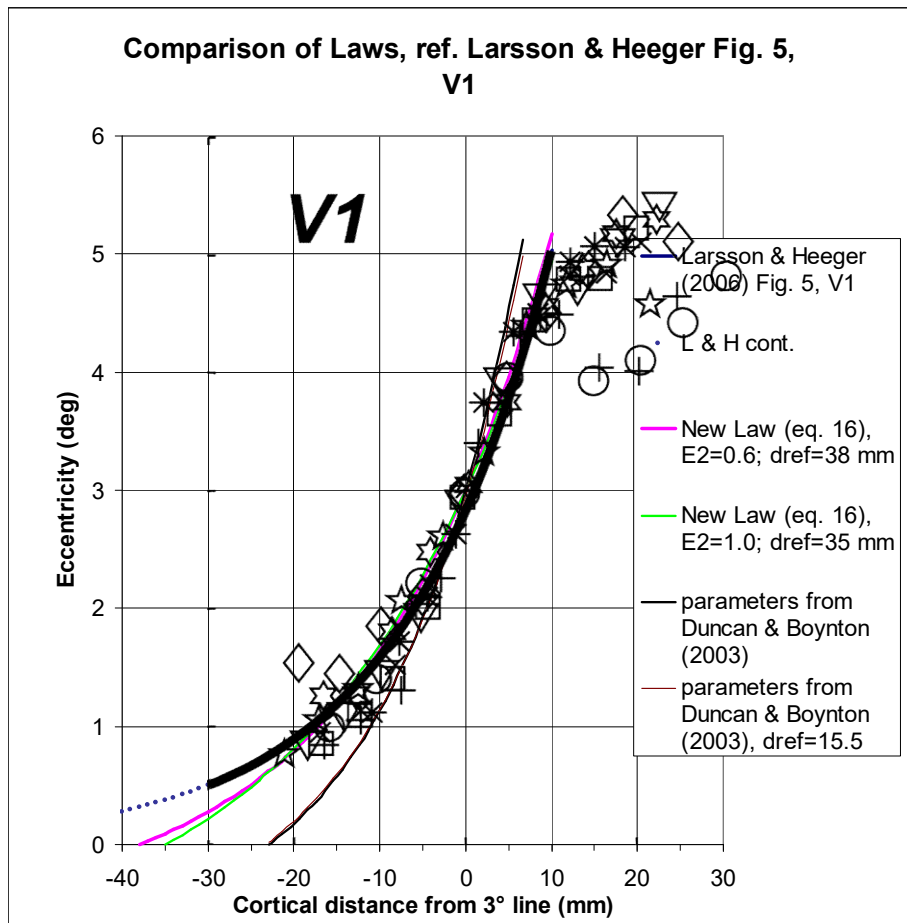
470

471   Figure 5. Comparison of conventional and improved analytic functions for describing the cortical location
472   function. Symbols show the retinotopic data for area V1 with reference location d_{ref} = 3° from Larsson and
473   Heeger (2006, Fig. 5) (symbols for nine subjects). Superimposed is the original fit (thick black line), according
474   to eq. (18) *(E = exp (a (d̂ + b)))* or eq. (19), i.e. a fit without a constant term. The blue dotted line continues
475   that fit to lower eccentricities; the fitted $E(\hat{d})$ function goes to (negative) infinite cortical distance, which is
476   physically meaningless. The pink and green line show graphs of the preferable eq. (16) that was derived
477   from integrating the inverse linear law (eq. 1).The equations are underconstrained if M_0 is not known; two
478   pairs of parameter choices are shown, [E_2 = 0.6°, d_{ref} = 38 mm] and [E_2 = 1.0°, d_{ref} = 35 mm], respectively.
479   The corresponding retinotopic centre's magnification factor M_0 can be calculated by eq. (17) as 35.4 mm/°
480   and 25.3 mm/° for the two cases, respectively. Black and brown line: $E(\hat{d})$ function with parameters derived
481   by Duncan & Boynton (2003), M_0 = 18.5 mm/° and E_2 = 0.831° (black), and with d_{ref} = 15.5 mm (brown) for
482   comparison (discussed in the next section). Note that, by definition, the curves from Larsson & Heeger pass
483   through the 3° point at $\hat{d}$ = 0 mm. Note also that, according to the authors, the data beyond ~10 mm were
484   biased and can be disregarded.

485   The pink and the green curve in Figure 5 are two examples for a fit of the equation with a
486   constant term (i.e., for eq. 16). Note that the equations are underconstrained unless either
487   the location of the retinotopic centre or the central CMF M_0 are known. The pink curve uses

15

488   E_2 = 0.6° and d_{ref} = 38 mm, and the green curve E_2 = 1.0° and d_{ref} = 35 mm. Apparently,
489   smaller E_2 values go together with larger d_{ref} values for a similar shape. Within the range of
490   the data set, the two curves fit about equally well; the pink curve is slightly more curved (a
491   smaller E_2 is accompanied by more curvature). Below about 1° eccentricity, i.e. around half
492   way between the 3° point and the retinotopic centre, the two curves deviate markedly from
493   the original fit. The new curves fit the data better there than the original and, in particular,
494   reach a retinotopic centre. Of the two, the pink curve (with E_2 = 0.6°) reaches the centre at
495   38 mm from the 3° point, and the green curve at 35 mm.

496   The centre cortical magnification factor, M_0, for the two curves can be derived from eq. (17),
497   giving a value of 35.4 mm/° and 25.3 mm/°, respectively. These two estimates differ
498   substantially from one another – by a factor of 1.4 – even though there is only a 3-mm
499   difference of the assumed location of the retinotopic centre. This illustrates the large effect
500   of the estimate for the centre's location on the foveal magnification factor, M_0. It also
501   illustrates the importance of a good estimate for that location.

502   There is a graphic interpretation of the foveal magnification factor M_0 in these graphs. From
503   eq. (6) one can derive that M_0^{-1} is equal to the function's slope at the retinotopic centre.
504   Thus, if the function starts more steeply (as does the green curve compared to the pink one),
505   M_0^{-1} is higher and thus M_0 is smaller.

506   The figure also shows two additional curves (black and brown), depicting data from Duncan
507   & Boynton (2003), which are discussed below. To better display the various curves' shapes,
508   they are shown again in Figure 6 but now without the data symbols. Figure 6 also includes an
509   additional graph, depicting the exponential function E = exp(0.063($\hat{d}$ + 36.54)) reported by
510   Engel et al. (1994, 1997). In it, $\hat{d}$ is again the cortical distance in millimetres but this time
511   measured from the 10° representation. E, as before, is the visual field eccentricity in
512   degrees. For comparison with the other curves, the curve is shifted (by 19.1 mm cortical
513   distance) on the abscissa, to show the distance from the 3° point. The curve runs closely with
514   that of Larsson & Heeger (2006) and shares its difficulties.
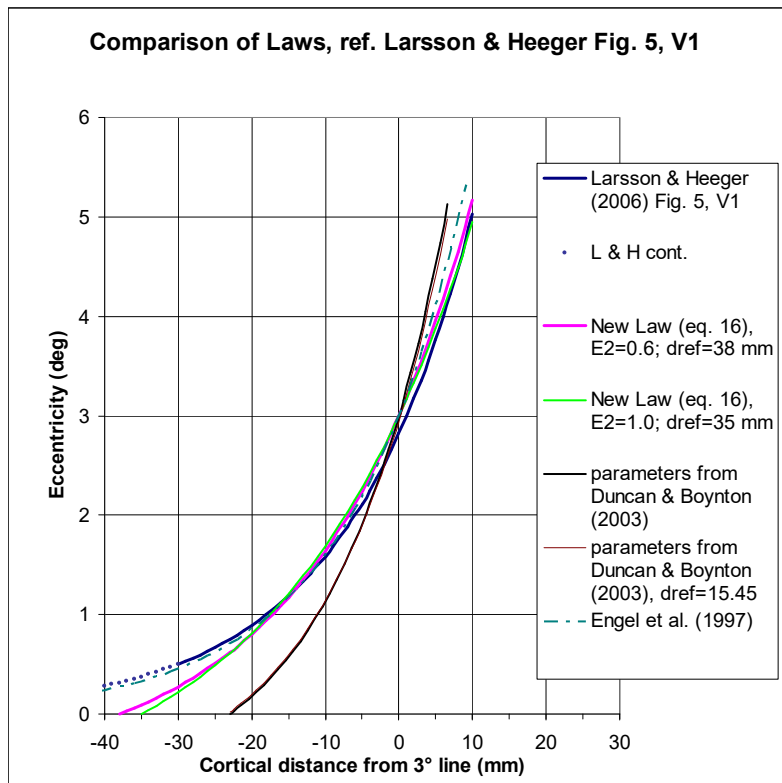
Figure 6. Same as Figure 5 but without the data symbols, for better visibility of the curves. The additional dash-dotted curve next to that of Larsson & Heeger's depicts the equation by Engel et al. (1997).

2.4.2 The approach of Duncan & Boynton (2003)

In addition to the curves just discussed, Figure 5 and Figure 6 show a further $E(\hat{d})$ function that is based on the results of Duncan & Boynton (2003). That function obviously differs quite a bit from the others in the figure and it is thus worthwhile studying how Duncan & Boynton (2003) derived these values. The paper takes a somewhat different approach for estimating the retinotopic mapping parameters for V1 than the one discussed before.

As a first step in Duncan & Boynton's paper, the locations of the lines of equal eccentricity are estimated for five eccentricities (1.5°, 3°, 6°, 9°, 12°) in the central visual field, using the equation $w = k * \log(z + a)$. The function looks similar to the ones discussed above, except that z is now a complex variable that mimics the visual field in the complex plane. On the horizontal half-meridian (where z is real-valued) that is equivalent to eq. (6) in the present paper, i.e., to an $E(d)$ function that includes a constant term (here parameter a) in the log's argument and with the retinotopic centre as the reference. At these locations, the authors then estimate the size of the projection of several 1°-patches of visual space (see their Fig. 3; this is where they differ in their methodology from other approaches). By definition, these sizes are the cortical magnification factors M_i at the corresponding locations. Numerically, these sizes are then plotted vs. eccentricity in the paper's Fig. 4 (reproduced in Figure 7A). Note that this is not readily apparent from the paper, since both the graph and the accompanying figure caption state something different. In particular the y-axis is labelled incorrectly (as is evident from the accompanying text). For clarity, therefore, Figure 7B here plots these data with a corrected label and on a linear y-axis.

17

540
541
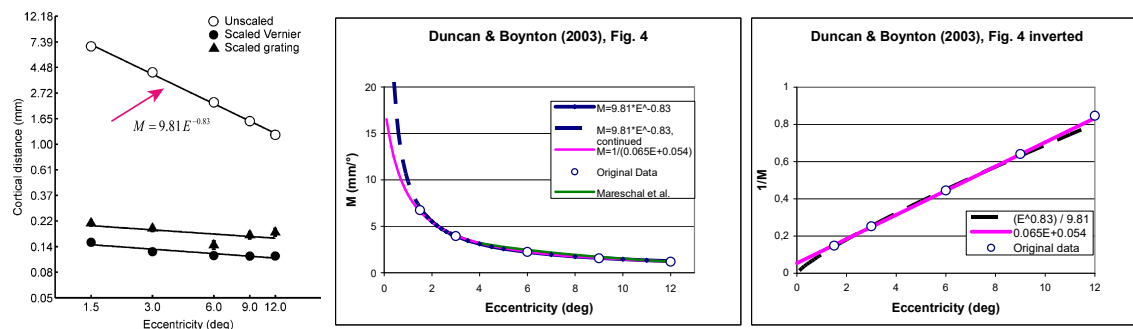
Figure 7. Duncan & Boynton's (2003) Fig. 4, showing the cortical magnification factor's variation with eccentricity. (A) Original Fig. 4. The open symbols follow a power function (note the double-linear coordinates). (B) Redrawn on a linear y-axis and with a *corrected* y-axis label (M in mm/°). Open circles show the original data. Note that the equation used in (A) and proposed earlier in the paper (p. 662), $M = 9.81*E^{-0.83}$, predicts an *infinite* foveal magnification factor, shown as the blue curve (with blue diamonds for visibility). In contrast, the inverse-linear fit $M^{-1} = 0.065\,E + 0.054$ proposed later in the paper (p. 666) fits the data equally well in the measured range of 1.5° to 12° but in contrast predicts a reasonable foveal magnification factor M_0 of 18.5 mm/°. The E_2 value for the latter equation is $E_2 = 0.83$. The additional green curve shows an equation by Mareschal et al. (2010) (see next section). (C) The inverse of the same functions. Note the slight but important difference at 0° eccentricity, where the original curve is zero and its inverse is thus undefined, whilst the linear function is *non-zero* and its inverse thus well-defined.

The authors next fit a power function to those data, stated as $M = 9.81*E^{-0.83}$ for the cortical magnification factor (note the double-logarithmic coordinates in 7A). There is more confusion, however, because it is said that, from such power functions, the foveal value can be derived by extrapolating the fit to the fovea (p. 666). That cannot be the case, however, since, by the definition of a power function (including those used in the paper), there is no constant term. The function therefore goes to infinity towards the fovea centre, as shown in Figure 7B (dashed line). Furthermore, E_2, which is said to be derived in this way in the paper, cannot be derived from a nonlinear function (because the E_2 concept requires a linear or inverse-linear function). The puzzle is resolved with a reanalysis of Duncan & Boynton's Fig. 4. It reveals how the foveal value and the connected parameter E_2 were, in fact, derived: as an inverse-linear function which fits the data equally well in the measured range of 1.5° – 12° eccentricity (Figure 7B and 7C, continuous line; note the slight but crucial difference in 7C the retinotopic centre). From that function, the foveal value and E_2 are readily derived. Indeed, the two values correspond to the values given in the paper.

The distance of the isoeccentricity lines from the retinotopic centre is not specified in Duncan & Boynton (2003). We can derive it from eq. (17), though, because M_0 and E_2 are fixed:

$$d_{ref} = M_0 \beta E_2 . \tag{20}$$

With the authors' parameters ($M_0 = 18.5$ mm/° and $E_2 = 0.83$), the scaling factor β in that equation comes out as $\beta = 1.03$ (from eq. 16). From that, $d_{ref} = d_{1.5°} = 15.87$ mm. As a further check, we can also derive a direct estimate of d_{ref} from their Fig. 3. For their subject ROD, for example, the 1.5° line is at a distance of $d_{1.5°} = 15.45$ mm on the horizontal meridian. That value is only very slightly smaller than the one derived above. For illustration, Figure 5 and Figure 6 in the previous section also contain a graph for that value (thin black line). Conversely, with d_{ref} given, M_0 can be derived from eq. (17) (or eq. 20), which gives a slightly smaller value of $M_0 = 18.0$ mm/°. The two curves are hardly distinguishable; thus, as

18

579   previously stated, d_{ref} and M_0 interact, with different value-pairs resulting in similarly good
580   fits.

581   In summary, the parameters in Duncan & Boynton's (2003) paper: M_0 = 18.5 mm/° and
582   E_2 = 0.83, are supported by direct estimates of the size of 1°-projections. They are taken at
583   locations estimated from a set of mapping templates, which themselves are derived from a
584   realistic distance-vs.-eccentricity equation. The paper provides another good example how
585   the linear concept for the magnification function can be brought together with the
586   exponential (or logarithmic) location function. The estimate of M_0 comes out considerably
587   lower than in more recent papers (e.g. Schira et al., 2009; see Figure 8 below). Possibly the
588   direct estimation of M at small eccentricities is less reliable than the approach taken in those
589   papers.

590   2.4.3 Mareschal, Morgan & Solomon (2010)

591   Figure 7 shows an additional curve from a paper by Mareschal et al. (2010) on cortical
592   distance, who base their cortical location function partly on the equation of Duncan &
593   Boynton (2003). Mareschal et al. (2010) state their location function as

594    $$M'(E) = \begin{cases} (0.065E + 0.054)^{-1} & E < 4° \\ 5.72 - \log_{1.73}(E) & E > 4° \end{cases} \tag{21}$$

595   The upper part of the equation is that of Duncan & Boynton (pink curve) and is used below
596   an eccentricity of 4°. The green continuous line shows Mareschal's log equation above 4°,
597   and the dashed line shows how the log function would continue for values below 4°. As in
598   the previous examples, the latter is not meaningful and is undefined at zero eccentricity,
599   which is why Mareschal et al. switched to the inverse-linear function (i.e. the pink curve) at
600   that point. The problem at low eccentricity is apparent in Fig. 9 of their paper where the x-
601   axis stops at ½ deg, so the anomaly is not fully seen. For their analysis, the switch of
602   functions is not relevant since eccentricities other than 4° and 10° were not tested. However,
603   the example is added here to illustrate that the case distinction in eq. (21) could be avoided
604   with the new equations derived here.

605   2.4.4 An added exponent: Sereno et al. (1995)

606   To accommodate for a slight curvature in the inverse CMF function (Figure 2A), several
607   authors have suggested using a modestly nonlinear function for its modelling (Rovamo &
608   Virsu, 1979; Van Essen et al., 1984; cf. Table 1). One way to achieve this is using a power
609   function, i.e., adding an exponent to the linear function with a value slightly above 1:

610    $$M^{-1} = M_0^{-1} \cdot (1 + aE)^\alpha \tag{22}$$

611   Van Essen et al. (1984), e.g., use an exponent of 1.1. Following their lead, Sereno et al.
612   ((1995)) posit

613    $$M(r) = \frac{A}{(r + B)^C} \tag{23}$$

614   for the CMF, where A, B, and exponent C are free parameters, and r denotes eccentricity
615   along a radius (the equations are found in the paper's footnotes 24, 25, and 26). For the case
616    $C = 0$, the equation is reduced to the standard inverse-linear function (eq. 1). By integration,
617   they derive from that the cortical location function, called *mapping function D(r) = ∫ M(r)dr* in
618   their paper:

19

619 $$D(r) = \frac{A(r + B)^{1-C}}{1 - C} \quad \text{with } C \neq 0 \tag{24}$$

620   In their fits to the anatomical data, *C* comes out with values close to 1.

621   Note that both eq. (22) and (23) are well-defined and meaningful in the retinotopic centre
622   (*r*=0). Note also, however, that the exponent *(C)* must not be zero for the location function
623   (eq. 24). I.e., the location function is undefined for the inverse-linear CMF function. That
624   latter case is discussed in Sereno et al.'s Footnote 26, where *C* = 1; the cortical location
625   function is then said to converge to

626   *D(r) = A* log *[r + B].* (25)

627   (i.e., similar to eq. 5).

628   In that equation, however, lies the fatal error that led to the avoidance of the (much simpler)
629   logarithmic location function. On closer inspection and comparison to eq. (5), one can see
630   that, even though there is a constant term (namely *B*), the scaling factor for the independent
631   variable *r* is missing. The equation should be something like *D(r) = A* log *[Cr + B]*. Therefore, *B*
632   is effectively constrained to 1 because only then is *D(r=0)* = 0. In other words, the constant
633   term *B* is not actually a free parameter.

634   Interestingly, Sereno et al. (1995) are aware of the shortcomings of the latter equation. They
635   write, "Our data could also be fit with this equation, but only if we allowed B to be negative,
636   which results in a singularity (infinite magnification factor) before the center-of-gaze is
637   reached. A good fit without a singularity could only be achieved with *C* above 1". They
638   continue saying, "The combinations of parameters given here fit the cortical distance data
639   [i.e., referring to the location function] very closely but still give unrealistically large
640   estimates of cortical magnification at the exact center of the fovea [...], indicating that the
641   standard equation for M is inadequate to accurately describe cortical magnification in the
642   very center of the fovea in humans even with C > 1." What went unnoticed is that a simple
643   remedy would have been using the correct additive constant term and a scaling factor for *r*.

644   **2.4.5 Toward the retinotopic centre: Schira et al.**

645   As discussed above, predictions on the properties at the retinotopic centre depend critically
646   on determining its precise location and thus require data at small eccentricities. Schira, Tyler
647   and coworkers have addressed that problem in a series of papers (Schira et al., 2007; Schira,
648   Tyler, Breakspear, & Spehar, 2009; Schira et al., 2010) and provide detailed maps of the
649   centres of the early visual areas, down to 0.075° eccentricity. They also develop parametric,
650   closed analytical equations for the 2D maps. When considered for the horizontal direction
651   only, these equations correspond to those discussed above (eq. 1 and eq. 16/17) (the
652   equations differ on, and close to, the vertical meridian – Schira et al., 2007; Schira et al.,
653   2010 – but this is not relevant here).

654   Figure 8 shows magnification factors from Schira et al., 2009, Fig. 7A, with figure part B
655   showing their V1 data (red curve), but redrawn on double-linear coordinates. As can be
656   seen, the curve runs close to a hyperbola. Its inverse is shown in Figure 8C, which displays
657   the familiar, close-to-linear behaviour over a wide range, with a positive y-axis intercept that
658   corresponds to the value at the retinotopic centre, M_0^{-1}. From the regression line, M_0 and E_2
659   are readily obtained and are E_2 = 0.21° and M_0 = 47.6 mm, respectively. Interestingly, a
660   rather large value of M_0 is obtained compared to previous reports. Partly (as can also be
661   seen from the graph) that can be caused by a single, most peripheral point; the centrally

20

662   located values predict a somewhat shallower slope of the linear function. If one disregards
663   that point in the regression, one arrives at a slightly larger E_2 and smaller M_0 value: $E_2 = 0.33°$
664   and $M_0 = 34.8$ mm. The latter values might be the more accurate predictors for V1's central
665   point.
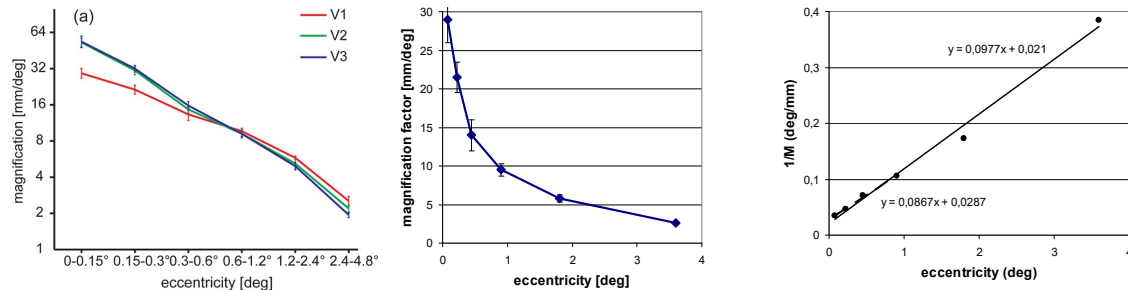
666

667   Figure 8. The cortical magnification factor's dependency on eccentricity from Schira, Tyler, Breakspear &
668   Spehar (2009, Fig. 7A). (A) Original graph. (B) V1 data for M, from Schira et al.'s graph but drawn on double-
669   linear coordinates, showing the hyperbola. (C) Resulting inverse factor, again on linear coordinates. The
670   regression line, $M^{-1} = 0.0977\,E + 0.021$, fits the whole set and predicts $E_2 = 0.21°$ and $M_0 = 47.6$ mm. The
671   regression equation $M^{-1} = 0.0867\,E + 0.0287$ is a fit to only the first four points and might be a better
672   predictor for the retinotopic centre, resulting in the values $E_2 = 0.33°$ and $M_0 = 34.8$ mm.

673   In summary, the derived equations provide a direct link between the nomenclature more
674   well-known in psychophysics and that in the neurophysiological literature on retinotopy.
675   They were applied to data for V1 (Fig. 2) but will work equally well for higher early visual
676   areas, including V2, V3, and V4 (cf. Larsson & Heeger, 2006, Fig. 5; Schira et al., 2009, Fig. 7).
677   M_0 is expected to be slightly different for the other areas (Schira et al., 2009, Fig. 7) and so
678   will likely be the other parameters.

679   **2.4.6 d_2 – a structural parameter to describe the cortical map**

680   As shown in Section 2.1, a newly defined structural parameter d_2 can be used to describe the
681   cortical location function very concisely (eq. 9 or 10). Parameter d_2 is the cortical
682   representation of Levi and Klein's E_2. That is, d_2 is the distance from the retinotopic centre,
683   measured in mm, corresponding to eccentricity E_2, which is where the foveal value doubles.
684   Eq. (8) can serve as a means to obtain an estimate for d_2. Essentially, d_2 is the product of M_0
685   and E_2 with a scaling factor. Table 2 gives a summary of d_2 estimates thus derived. The value
686   of $d_2 \approx 8$ mm with $E_2 = 0.33°$, based on Schira et al.'s (2009) data which go down to very low
687   eccentricities, might be the most accurate estimate currently given their sophisticated
688   methodology for assessing the map closely around the retinotopic centre.

689   Similar to what E_2 does for the linear or inverse-linear function – be it the anatomical CMF or
690   thresholds in a psychophysical task – d_2 concisely captures the properties of the map in a
691   single number. It is given in physical units (mm) and can thus be drawn directly into a
692   retinotopic map. E_2 can be (and has been) used as a summary measure for the CMF but is
693   not as well-suited because its units are in deg visual angle on the retina (or in the visual
694   field), i.e. needs to be translated to spatial, cortical units. Currently, typical characterisations
695   of the cortical map are done by drawing iso-eccentricity lines at several eccentricities (10°,
696   20°, 30°, etc.). In a similar way, a single d_2 line could be drawn on the cortical map, or d_2
697   could marked as a point on a radius. As a characteristic measure, d_2 could be used in many
698   ways, for comparison of the anisotropy in the cortical maps, between species, individuals,

699 gender, etc. Or indeed it could describe any other retinotopic map like those for V2 – V4 or
700 that for the LGN, the pulvinar, the reticular nucleus of the thalamus, once data are available.
701 Differences between d_2 show a difference in the architecture.

702 That said, d_2 shares certain limitations of E_2 (Strasburger et al., 2011, Fig. 11 and Table 3).
703 Like the latter, it relies on data in, and near, the retinotopic centre and can thus be expected
704 to be most meaningful at small to medium eccentricities. Its validity for describing the curve
705 at larger eccentricities further depends on the premise that location in the map results from
706 integrating the local magnification function, i.e., that local magnification factors "add up".
707 For the CMF, that appears to be the case, as evidenced by the good fit of location data
708 shown in Figure 5 and other log location functions in the literature. Yet for local properties
709 that are likely based on differences in neural wiring, like the colour channels studies in
710 D'Souza et al. (2016), that might not be the case. d_2, in those cases, will characterise the
711 function, but not its map.

712 Note in Table 2 that both the estimates for M_0 (the central CMF for V1) and E_2 vary quite a
713 bit between neuroanatomical studies. Except for Dougherty et al.'s (2003, Fig. 5) estimate,
714 current M_0 estimates are much larger than the old estimates of M_0 = 8.55 mm/° from Cowey
715 & Rolls (1974) or M_0 = 7.99 mm/° from Rovamo & Virsu (1979) (for more estimates of M_0,
716 see Strasburger et al., 2011, Table 5). At the same time, again except Dougherty et al. (2003,
717 Fig. 5), modern E_2 values for the CMF on the whole appear smaller than the old values
718 (Cowey & Rolls: 1.75°, Rovamo & Virsu: 3.0°). Since, in essence d_2 is the product of the two,
719 these variations in opposite directions are evened by d_2 which indeed varies less between
720 studies. This might be another reason why d_2 could be a more suitable structural parameter
721 for a retinotopic map than either M_0 or E_2 on its own.

Study	M_0 [mm/°]	E_2 [°]	d_2 [mm]	Curve
Larsson & Heeger (2006)	35.4	0.6	14.72	Fig. 4, pink
"	25.3	1.0	17.54	Fig. 4, green
Duncan & Boynton (2003)	18.5	0.831	10.66	Fig. 4, black
Schira, Tyler, Breakspear & Spehar (2009)	47.6	0.21	6.93	Fig. 7C
"	34.8	0.33	**7.96**	Fig. 7C, 2nd regression
Dougherty et al. (2003, Fig. 5)	7.4	3.67	18.8	Fig. 1C, pink (for V1)
D'Souza, Auer, Frahm, Strasburger & Lee (2016, Fig. 4)	32.32*	0.45	10.08	|L-M| Channel
"	32.32*	0.97	21.73	Lum Channel
"	32.32*	3.4	76.17	S Channel

722 Table 2. Values of the parameter d_2 from an analysis of data in several studies, by eq. (8): $d_2 = M_0 E_2 \ln(2)$. d_2
723 is the cortical representation of E_2 and characterizes the cortical location function in a single value.

724 *M_0 was not estimated in that paper; the mean of the preceding M_0 values (except Dougherty et al., 2003
725 which has an exceptionally low M_0) was used for the calculation instead.

3. Crowding and Bouma's Law in the cortex

727 The preceding sections were about the cortical location function; in the final section that
728 function will be applied to an important property of cortical organization: visual crowding.
729 Whereas, in the preceding, cortical *location* was the target of interest, in this section we are
730 concerned with cortical *distances*.

731   As reviewed in the introduction, MAR-like functions like acuity generally change in
732   peripheral vision in that *critical size* scales with eccentricity, so deficits can (mostly) be
733   compensated for by *M*-scaling (as, e.g. in Rovamo & Virsu, 1979). For crowding, in contrast,
734   target size plays little role (Strasburger et al., 1991; Pelli et al., 2004; Whitney & Levi, 2011).
735   Instead, the critical *distance* between target and flankers scales with eccentricity, though at
736   a different rate than MAR (Rosenholtz, 2016; Strasburger, 2020). This scaling characteristic
737   of crowding is known as Bouma's rule or Bouma's law (Bouma, 1970; Strasburger et al.,
738   1991; Pelli et al., 2004; Pelli & Tillman, 2008; Strasburger, 2020). The corresponding
739   distances in the primary cortical map are thus governed by *differences* of the cortical
740   location function as derived here in Section 2. Crowding's critical distance (or indeed any
741   distance, including acuity gap size) is thus, in a sense, a spatial derivative of location. Pattern
742   recognition, at even slight eccentricities, is governed by the crowding phenomenon and is
743   largely unrelated to visual acuity (or thus to cortical magnification) (Strasburger et al., 1991;
744   Pelli et al., 2004; Pelli et al., 2007; Pelli & Tillman, 2008; Strasburger & Wade, 2015). For
745   understanding crowding it is paramount to look at its cortical basis, since we know since
746   Flom, Weymouth, & Kahnemann (1963) that crowding is of cortical origin (as also
747   emphasized by Pelli, 2008).

748   A question that arises naturally in that context then is how the cortical equivalent of critical
749   crowding distance varies across the visual field. Klein & Levi (1987) were the first to consider
750   a related question, namely how the cortical distance for distance threshold in a vernier task
751   varies with eccentricity. They conclude that it is approximately constant. That conclusion was
752   based on the observation that taking the first derivative of Schwartz's (1980) log mapping
753   using the constancy assumption will result in the well-known inverse-linear cortical
754   magnification function. Conversely, their empirically determined position thresholds, when
755   mapped by an inverse-linear cortical magnification function (with an E_2 of 0.6), turned out
756   mostly constant across a wide range of eccentricities (cf. Klein & Levi's Fig. 5). Later, Duncan
757   and Boynton (2003), after estimating *M* based on Schwartz's (1980) log mapping and
758   applying that to obtain cortical distances (see Section 2.4.2), show that, for scaled vernier
759   tasks and scaled gratings, the cortical equivalents are again mostly constant (above 1.5°
760   eccentricity; 2003, Fig. 4). Similarly, with respect to the cortical distance for crowding's
761   critical distance, it has been proposed that it is likely a constant, with the same reasoning
762   Motter & Simoni, 2007; Pelli, 2008; Mareschal, Morgan, & Solomon, 2010; oddly, the original
763   source for the log mapping, Fischer, 1973, is not cited in the above papers).

764   Elegant as it seems as a take-home message, however, the constancy assumption is most
765   likely incorrect as a general rule and is only true at sufficiently large eccentricities. If stated
766   as a general rule, it rests on the same shortcut of equating linearity and proportionality, i. e.
767   the omission of the constant term that gave rise to those cortical location functions that
768   miss the retinotopic centre (Section 2.3). Based on the properties of the cortical location
769   function derived in Section 2, it will turn out that the critical cortical crowding distance
770   increases steeply within the fovea (where, e.g., reading mostly takes place) and reaches an
771   asymptote beyond perhaps 5° eccentricity, consistent with a constancy at sufficient
772   eccentricity. Accordingly, Pelli (2008) warns against extrapolating the constancy toward the
773   retinotopic centre. Remarkably (and to my pleasant surprise), after I had completed the
774   derivations it turned out that the analytic equation exposed below nicely agrees with those
775   presented by Motter & Simoni (2007, Fig. 7). In that figure, reproduced here in Figure 9B,
776   only the more peripheral data above about 10° show the presumed constancy.

777   Let us turn to the equations. Bouma (1970) stated what is now known as Bouma's law for
778   crowding (Strasburger, 2020):

779    $\delta_{space} = bE$, (26)

780   where δ_{space} is the free space between the patterns at the critical distance and b is a
781   proportionality factor. Bouma (1970) proposed an approximate value of b = 0.5 = 50%, which
782   is now widely cited, but he also mentioned that other proportionality factors might work
783   equally well; indeed, Pelli et al. (2004) have shown that b can take quite different values,
784   depending on the exact visual task. Yet even though the factor may be different between
785   tasks, the implied linearity of eq. (26) almost always holds up. The law could thus be restated
786   as saying that free space for critical spacing is proportional to eccentricity, with the
787   proportionality factor taking some value around 50% or 40%, depending on the task.

788   In today' literature it has become customary to state flanker distance not as free space but
789   as measured from the respective centres of target and flankers. The critical spacing then
790   remains largely constant across sizes as Tripathy & Cavanagh, 2002 and others have shown.
791   To restate Bouma's law for that centre-to-centre distance δ , let the target pattern have a
792   size S in the radial direction (e.g., *width* in the horizontal), so that $\delta = S + \delta_{space}$. Then eq.
793   (26) becomes

794    $\delta = bE + S$. (27)

795   This equation no longer represents proportionality yet is still linear in E. Importantly,
796   however, going from Bouma's equation (eq. 26) to that in eq. (27) reflects adding the
797   constant term that we talked about in the preceding sections. And formally, that equation
798   (27) is analogous to size scaling as in. (2). Analogously to Levi and Klein's E_2 we therefore
799   introduce a parameter $\hat{E}_2$ for crowding, as *the* eccentricity where the *foveal value of critical
800   distance doubles*. Denoting the foveal value of critical distance by δ_0 , we get, from eq. (27):

801    $\delta = \delta_0 (E / \hat{E}_2 + 1)$. (28)

802   Obviously, that equation is analogous to eq. (1) and (2) that we started out with; it describes
803   how critical distance in crowding is linearly dependent on (but is not proportional to)
804   eccentricity in the visual field. In this respect, it thus behaves like acuity and many other
805   spatial visual performance measures, just with a different slope and axis intercept.

806   With the equations derived in the preceding sections, we can now derive the critical
807   crowding distance in the cortical map, i.e. the cortical representation of critical distance in
808   the visual field. Let us denote that distance by κ (kappa). By definition, it is the difference
809   between the map locations for the target and a flanker at the critical distance in the
810   crowding task: $\kappa = d_f - d_t$. The two cortical locations d_f and d_t are, in turn, obtained from
811   the mapping function, which is given by inverting eq. (6) above:

812    $d = M_0 E_2 \ln\left(1 + E\!\big/\!E_2\right)$, (with $E \geq 0$). (29)

813   As before, d is the distance of the location in the cortical map from the retinotopic centre.
814   So, critical distance κ for crowding in the retinotopic map is the difference of the respective
815   d values for target and flanker, $\kappa = d_f - d_t$:

816
$$\kappa = M_0 E_2 \ln\left(1 + \frac{E_f}{E_2}\right) - M_0 E_2 \ln\left(1 + \frac{E_t}{E_2}\right) = M_0 E_2 \ln\frac{\left(1 + \frac{(E_t + \delta_0(E_t/\hat{E}_2 + 1))}{E_2}\right)}{\left(1 + \frac{E_t}{E_2}\right)}$$ (30)

817   (by eq. 29 and 28), where E_t and E_f are the respective eccentricities at which target and
818   flanker are located.

819   After simplifying and setting target eccentricity $E_t = E$ for generality, this becomes

820
$$\kappa = M_0 E_2 \ln\left(1 + \frac{\delta_0}{E_2} \frac{(1 + E/\hat{E}_2)}{(1 + E/E_2)}\right).$$ (31)

821   Note that we stated that equation previously (Strasburger & Malania, 2013, eq. 13, and
822   Strasburger et al., 2011, eq. 28), but, alas, incorrectly: a factor was missing.

823   To explore this function, its graph is shown in Figure 9A and we look at two special cases. In
824   the retinotopic centre, equation (31) predicts a critical distance κ_0 in the cortical map of

825
$$\kappa_0 = M_0 E_2 \ln\left(1 + \frac{\delta_0}{E_2}\right).$$ (32)

826   With increasing eccentricity, κ departs from that foveal value and increases, depending on
827   the ratio $E_2 / \hat{E}_2$ (provided $E_2 > \hat{E}_2$ which can be reasonably assumed; Latham & Whittaker
828   (1996; Strasburger, 2020). Numerator and denominator are the E_2 values for the location
829   function and the crowding function, respectively (eq. 1 vs. eq. 28). They are generally
830   different, so their ratio is not unity.

831   With sufficiently large eccentricity, the equation converges to

832
$$\lim_{E \to \infty} \kappa = M_0 E_2 \ln\left(1 + \frac{\delta_0}{\hat{E}_2}\right).$$ (33)

833   The expression is shown as dashed line in Figure 9A. It is identical to that for the foveal value
834   in eq. (33) except that E_2 is now replaced by the corresponding value $\hat{E}_2$ for crowding.
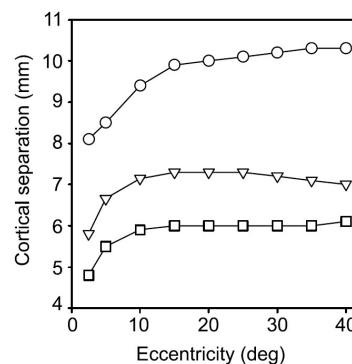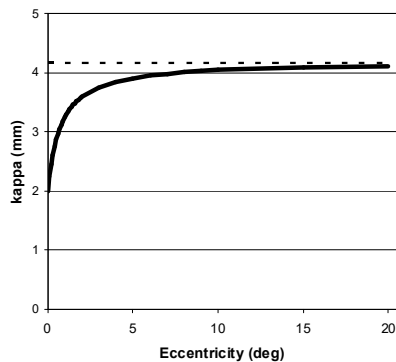

25

Figure 9. (A) Graph of eq. (31) with realistic values for M_0, E_2, $\hat{E}_2$, and δ_0. The value of E_2 for M^{-1} was chosen as $E_2 = 0.8°$ from Dow, Snyder, Vautin, & Bauer, 1981 (as cited in Levi et al., 1985, or Strasburger et al., 2011, Table 4). $M_0 = 29.1$ mm was chosen to give a good fit with this E_2 in Fig. 2. Foveal critical distance was set to $\delta_0 = 0.1°$ from Siderov, Waugh, & Bedell, 2013, 2014. An $\hat{E}_2 = 0.36°$ would obtain with this δ_0 and the value of $\delta_{4°} = 1.2°$ in Strasburger et al., 1991; it also serves as an example for being a clearly different value than E_2 for the cortical magnification factor, to see the influence of the $E_2 / \hat{E}_2$ ratio on the graph. Cortical critical distance κ starts from the value given in eq. (32) for the fovea centre (around 2 mm) and converges to the value in eq. (33). (B) Cortical critical distance for crowding from Motter & Simoni (2007, Fig. 7), showing the qualitative similarity for the dependency. The curves are effectively based on Duncan & Boynton's (2003) inverse-linear equation (see Figure 7B above, pink curve), which implies $M_0 = 18.5$ mm/° und $E_2 = 0.83°$. The middle curve (triangles) is comparable to the curve in (A). The different asymptote in (B) stems from a different M_0.

835 Importantly, note that *kappa* varies substantially around the centre, by around two-fold
836 between the centre and 5° eccentricity with realistic values of E_2 and $\hat{E}_2$. This, as said above,
837 is at odds with the conjecture that the cortical critical crowding distance is basically a
838 constant (Motter & Simoni, 2007; Pelli, 2008; Mareschal et al., 2010). Pelli (2008) presented
839 a mathematical derivation for the constancy, very similar to the one presented above –
840 based on Bouma's law and Schwartz' (1980) logarithmic mapping function. The discrepancy
841 arises from the underlying assumptions: Pelli used Bouma's law as proportionality, i.e., in its
842 simplified form stated in eq. (26) (its graph passing through the origin). The simplification
843 was done on the grounds that the error is small outside the retinotopic centre and plays
844 little role; the paper appropriately warns that additional provisions must be made at small
845 eccentricities. Schwartz's (1980) (simplified) mapping function was consequently also used in
846 its simplified form (without the constant term), for the same reason. With these
847 simplifications the critical distance in the cortex indeed turns out as simply a constant.

848 As should be expected, at sufficiently high eccentricities κ is close to constant in the
849 derivations given above (Figure 9). These equations (eq. 31–33) can thus be seen as a
850 generalization of Pelli's result that now also covers the (obviously important) case of central
851 vision.

852 For comparison, Figure 9B shows critical crowding spacing on the cortical map from a paper
853 on visual search by Motter & Simoni (2007). Note that the shown curves, though inspired by
854 their experimental search data, are not based on these but are based on a cortical-surface
855 model (shown in their Fig. 1), obtained by M-scaling visual distances. Critical distances are
856 assumed to follow Bouma's law, with a Bouma factor of ½. M-scaling is by Duncan &
857 Boynton's (2003) inverse-linear equation ($1/M(w) = 0.065w + 0.054$; shown here in Figure 7B
858 above, pink curve). The figure's basis is thus the same as in the present paper and effectively
859 shows Bouma's law mapped onto the cortex. The three curves refer to different flanker
860 location and reflect crowding asymmetry (see Strasburger, 2020, for review) (upper curve:
861 peripheral flanker, lower curve: central flanker); the middle curve is is for equal-eccentricity
862 flanker distances and is the one comparable to the curve in (A). Duncan & Boynton's
863 equation implies $M_0 = 18.5$ mm/° and $E_2 = 0.83°$ (cf. Table 2 above). That E_2 is similar to that
864 assumed in Figure 9A; M_0 is different. As we have seen in eq. (33), the asymptote depends
865 on these two values. The different asymptote in 9B thus stems from the different M_0.

866 Pelli & Tillman (2008, Online Supplement) derive a value of 6 mm for the asymptote. It is
867 based on eq. (18) above, as reported by Larsson & Heeger (2006), and a Bouma factor of 0.4.

868 An interesting (though unrealistic) special case of eq. (31) is the one in which E_2 and $\hat{E}_2$ are
869 equal. κ is then a constant, as Pelli (2008) predicted. Its value in that case would be simply
870 given by

871 $$\kappa = M_0 E_2 \ln\left(1 + \frac{\delta_0}{E_2}\right), \text{ for } E_2 = \hat{E}_2.$$ (34)

872 On a different note, equations (31)–(34) have M_0 as a scaling factor and, as said before, M_0
873 appears to be more difficult to determine empirically. However, M_0 can be replaced, as
874 shown above. From eq. (17) we know that

875 $$M_0 E_2 = \frac{d_{ref}}{\beta},$$ (35)

876 which, by the definition of β, takes a particularly simple form when we choose d_2 (the
877 cortical equivalent of E_2) as the reference:

878 $$M_0 E_2 = \frac{d_2}{\ln 2}$$ (36)

879 (this is the same as eq. 8a). We can then rewrite the equation for the critical cortical
880 crowding distance (eq. 31) as

881 $$\kappa = \frac{d_2}{\ln 2} \ln\left(1 + \frac{\delta_0}{E_2} \frac{(1 + E/\hat{E}_2)}{(1 + E/E_2)}\right).$$ (37)

882 Similarly, the two special cases given in eq. (32) and (33) become

883 $$\kappa_0 = \frac{d_2}{\ln 2} \ln\left(1 + \frac{\delta_0}{E_2}\right)$$ (38)

884 and

885 $$\lim_{E \to \infty} \kappa = \frac{d_2}{\ln 2} \ln\left(1 + \frac{\delta_0}{\hat{E}_2}\right).$$ (39)

886 Values for d_2 derived from the literature by eq. (36) that could be plugged into eq. (38) and
887 (39) *were provided in Table 2 above*. These two equations ((38) and (39)), for the retinotopic
888 centre and eccentricities above around 5°, respectively, could lend themselves for
889 determining critical crowding distance in the cortex.

890 In summary for the cortical crowding distance, the two well-established linear eccentricity
891 laws –for cortical magnification in neuroscience and critical crowding distance in
892 psychophysics –together with Fischer's (1973) or Schwartz's (1977; 1980) equally well-
893 established logarithmic mapping rule, predict a highly systematic behaviour of crowding's
894 critical distance in the cortical map. Given the very similar mappings in areas V2, V3, V4
895 (Larsson & Heeger, 2006; Schira et al., 2009), that relationship can be expected to be similar
896 in those areas as well (see Figure 9A for a graph). Since the equations for crowding follow
897 mathematically, they should work well there with suitable E_2 values inserted. Thus, direct

27

898 confirmations of their behaviour can cross-validate mapping models and might shed light on
899 the cortical mechanisms underlying crowding.

4. Outlook

901 Where does this leave us? The early cortical visual areas are very regularly organized and
902 their spatial maps appear to be pretty similar. Yet variation of perceptual performance
903 across the visual field differs widely between visual tasks, as highlighted by their respective,
904 widely differing E_2 values. For cortical magnification, in contrast, E_2 estimates appear quite
905 similar to each other. It is not yet clear how different spatial scalings in psychophysics can
906 emerge from a largely uniform cortical architecture when there can be only one valid
907 location function on any radius. The equivalence between psychophysical E_2 and the cortical
908 location function in the preceding equations thus likely only hold for a single E_2, presumably
909 the one pertaining to low-level tasks that are somehow connected to stimulus size. $\hat{E}_2$ for
910 critical crowding distance would be an example for a psychophysical descriptor that is
911 decidedly not related to stimulus size (Tripathy & Cavanagh, 2002; Pelli et al., 2004); it rather
912 reflects location differences. The underlying cortical architecture that brings about
913 psychophysical E_2 values different from that of the CMF (like $\hat{E}_2$) could be neural wiring
914 differences, within or between early visual areas, underneath a similar topography.

915 The link between the (local) CMF function and the (global) cortical location function derived
916 here rests on the assumption of spatial additivity – that local distances add-up to global
917 distances and the location function is thus the integral of the CMF function. E_2 values
918 different from that of the CMF thus do not translate to a location function. When two
919 different E_2 values act together, as in crowding, nonlinear functions as those in Figure 9
920 arise.

921 To go further, one of the basic messages of the cortical-magnification literature is the
922 realization that by M-scaling stimulus size some, but not all, performance variations are
923 equalised across the visual field. In parameter space, these other variables can be said to be
924 *orthogonal* to target size. Pattern contrast is such a variable (Strasburger, Rentschler, &
925 Harvey, 1994) which needs to be scaled independently from size to equalize performance in
926 pattern recognition. Temporal resolution is another example (Poggel, Calmanti, Treutwein, &
927 Strasburger, 2012). Again, differing patterns of connectivity between retinal cell types, visual
928 areas, and along different processing streams likely underlie these performance differences.
929 The aim of the present paper is just to point out that a *common spatial location function*
930 underlies the early cortical architecture that can be described by a unified equation. This
931 equation includes the fovea including the retinotopic centre, and has parameters that are
932 common in psychophysics and physiology.

Acknowledgements

References

Aubert, H. R., & Foerster, C. F. R. (1857). Beiträge zur Kenntniss des indirecten Sehens. (I). Untersuchungen über den Raumsinn der Retina. *Archiv für Ophthalmologie, 3*, 1-37.

Bouma, H. (1970). Interaction effects in parafoveal letter recognition. *Nature, 226*, 177-178.

Cowey, A., & Rolls, E. T. (1974). Human cortical magnification factor and its relation to visual acuity. *Experimental Brain Research, 21*, 447-454.

D'Souza, D. V., Auer, T., Strasburger, H., Frahm, J., & Lee, B. B. (2016). Dependence of chromatic response in V1 on visual field eccentricity and spatial frequency: an fMRI study. *Journal of the Optical Society of America A, 33*(3), A53-A64.

Daniel, P. M., & Whitteridge, D. (1961). The representation of the visual field on the cerebral cortex in monkeys. *Journal of Physiology, 159*, 203-221.

Dougherty, R. F., Koch, V. M., Brewer, A. A., Fischer, B., Modersitzki, J., & Wandell, B. A. (2003). Visual field representations and locations of visual areas V1/2/3 in human visual cortex. *Journal of Vision, 3*(10), 586-598.

Dow, B. M., Snyder, R. G., Vautin, R. G., & Bauer, R. (1981). Magnification factor and receptive field size in foveal striate cortex of the monkey. *Experimental Brain Research, 44*, 213-228.

Duncan, R. O., & Boynton, G. M. (2003). Cortical magnification within human primary visual cortex. Correlates with acuity thresholds. *Neuron, 38*, 659-671.

Engel, S. A., Glover, G. H., & Wandell, B. A. (1997). Retinotopic organization in human visual cortex and the spatial precision of functional MRI. *Cerebral Cortex, 7*, 181–192.

Engel, S. A., Rumelhart, D. E., Wandell, B. A., Lee, A. T. L., Glover, G. H., Chichilnisky, E.-J., et al. (1994). fMRI of human visual cortex. *Nature, 369*(6481), 525.

Fischer, B. (1973). Overlap of receptive field centers and representation of the visual field in the cat's optic tract. *Vision Research, 13*, 2113-2120.

Flom, M. C., Weymouth, F. W., & Kahnemann, D. (1963). Visual resolution and contour interaction. J. Opt. Soc. Am. 53, 1026-1032.

Foster, D. H., Thorson, J., McIlwain, J. T., & Biederman-Thorson, M. (1981). The fine-grain movement illusion: A perceptual probe of neural connectivity in the human visual system. *Vision Research, 21*, 1123-1128.

Harvey, B. M., & Dumoulin, S. O. (2011). The relationship between cortical magnification factor and population receptive field size in human visual cortex: Constancies in cortical architecture. *The Journal of Neuroscience, 31*(38), 13604 –13612.

Harvey, L. O., Jr., & Pöppel, E. (1972). Contrast sensitivity of the human retina. *American Journal of Optometry and Archives of the American Academy of Optometry, 49*, 748-753.

Horton, J. C., & Hoyt, W. F. (1991). The representation of the visual field in human striate cortex. A revision of the classic Holmes map. *Archives of Ophthalmology, 109*(6), 816-824.

Klein, S. A., & Levi, D. M. (1987). Position sense of the peripheral retina. *Journal of the Optical Society of America A, 4*(8), 1543-1553.

Larsson, J., & Heeger, D. J. (2006). Two retinotopic visual areas in human lateral occipital cortex. *The Journal of Neuroscience, 26*(51), 13128-13142.

Latham, K., & Whitaker, D. (1996). Relative roles of resolution and spatial interference in foveal and peripheral vision. *Ophthalmic and Physiological Optics, 16*, 49-57.

Levi, D. M., Klein, S. A., & Aitsebaomo, A. P. (1984). Detection and discrimination of the direction of motion in central and peripheral vision of normal and amblyopic observers. *Vision Research, 24*, 789-800.

Levi, D. M., Klein, S. A., & Aitsebaomo, A. P. (1985). Vernier acuity, crowding and cortical magnification. *Vision Research, 25*, 963-977.

Mäkelä, P., Näsänen, R., Rovamo, J., & Melmoth, D. (2001). Identification of facial images in peripheral vision. *Vision Research, 41*, 599–610.

Mareschal, I., Morgan, M. J., & Solomon, J. A. (2010). Cortical distance determines whether flankers cause crowding or the tilt illusion. *Journal of Vision, 10*(8), 13:11-14.

990 Motter, B. C., & Simoni, D. A. (2007). The roles of cortical image separation and size in active visual
991   search performance. *Journal of Vision, 7(2):6*, 1–15.
992 Nandy, A. S., & Tjan, B. S. (2012). Saccade-confounded image statistics explain visual crowding.
993   *Nature Neuroscience, 15*(3), 463-471.
994 Oehler, R. (1985). Spatial interactions in the rhesus monkey retina: a behavioural study using the
995   Westheimer paradigm. *Experimental Brain Research, 59*, 217-225.
996 Osterberg, G. (1935). Topography of the layer of rods and cones in the human retina. *Acta
997   Ophthalmologica. Supplement, 6-10*, 11-96.
998 Pelli, D. G. (2008). Crowding: a cortical constraint on object recognition. *Current Opinion in
999   Neurobiology, 18*, 445–451.
1000 Pelli, D. G., Palomares, M., & Majaj, N. J. (2004). Crowding is unlike ordinary masking: Distinguishing
1001   feature integration from detection. *Journal of Vision, 4*(12), 1136-1169.
1002 Pelli, D. G., & Tillman, K. A. (2008). The uncrowded window of object recognition. *Nature
1003   Neuroscience, 11*(10), 1129-1135 (plus online supplement).
1004 Pelli, D. G., Tillman, K. A., Freeman, J., Su, M., Berger, T. D., & Majaj, N. J. (2007). Crowding and
1005   eccentricity determine reading rate. *Journal of Vision, 7*(2).
1006 Poggel, D. A., Calmanti, C., Treutwein, B., & Strasburger, H. (2012). The Tölz Temporal Topography
1007   Study: Mapping the visual field across the life span. Part II: Cognitive factors shaping visual field
1008   maps. *Attention, Perception & Psychophysics, 74*, 1133-1144.
1009 Pöppel, E., & Harvey, L. O., Jr. (1973). Light-difference threshold and subjective brightness in the
1010   periphery of the visual field. *Psychologische Forschung, 36*, 145-161.
1011 Rovamo, J., & Virsu, V. (1979). An estimation and application of the human cortical magnification
1012   factor. *Experimental Brain Research, 37*, 495-510.
1013 Rovamo, J., Virsu, V., & Näsänen, R. (1978). Cortical magnification factor predicts the photopic
1014   contrast sensitivity of peripheral vision. *Nature, 271*, 54-56.
1015 Schira, M. M., Tyler, C. W., Breakspear, M., & Spehar, B. (2009). The foveal confluence in human
1016   visual cortex. *The Journal of Neuroscience, 29* (July 15), 9050 –9058.
1017 Schira, M. M., Tyler, C. W., Spehar, B., & Breakspear, M. (2010). Modeling magnification and
1018   anisotropy in the primate foveal confluence. *PLoS Computational Biology, 6*(1), e1000651.
1019 Schira, M. M., Wade, A. R., & Tyler, C. W. (2007). Two-dimensional mapping of the central and
1020   parafoveal visual field to human visual cortex. *Journal of Neurophysiology [Epub ahead of print],
1021   97*(6), 4284-4295.
1022 Schwartz, E. L. (1977). Spatial mapping in the primate sensory projection: Analytic structure and
1023   relevance to perception. *Biological Cybernetics, 25*, 181-194.
1024 Schwartz, E. L. (1980). Computational anatomy and functional architecture of striate cortex: A spatial
1025   mapping approach to perceptual coding. *Vision Research, 20*, 645-669.
1026 Sereno, M. I., Dale, A. M., Reppas, J. B., Kwong, K. K., Belliveau, J. W., Brady, T. J., et al. (1995).
1027   Borders of multiple visual areas in humans revealed by functional magnetic resonance imaging.
1028   *Science 268*, 889–893.
1029 Siderov, J., Waugh, S. J., & Bedell, H. E. (2013). Foveal contour interaction for low contrast acuity
1030   targets. *Vision Research, 77*, 10–13.
1031 Siderov, J., Waugh, S. J., & Bedell, H. E. (2014). Foveal contour interaction on the edge: response to
1032   'letter-to-the-editor' by Drs. Coates and Levi. *Vision Research, 96*, 145-148.
1033 Slotnick, S. D., Klein, S. A., Carney, T., & Sutter, E. E. (2001). Electrophysiological estimate of human
1034   cortical magnification. *Clinical Neurophysiology, 112*(7), 1349-1356.
1035 Strasburger, H. (2020). Seven myths on crowding and peripheral vision. *i-Perception, 11*(3), 1-46.
1036 Strasburger, H., Harvey, L. O. J., & Rentschler, I. (1991). Contrast thresholds for identification of
1037   numeric characters in direct and eccentric view. *Perception & Psychophysics, 49*, 495-508.
1038 Strasburger, H., & Malania, M. (2013). Source confusion is a major cause of crowding. *Journal of
1039   Vision, 13*(1), 1-20.
1040 Strasburger, H., Rentschler, I., & Harvey, L. O., Jr. (1994). Cortical magnification theory fails to predict
1041   visual recognition. *European Journal of Neuroscience, 6*, 1583-1588.

1042 Strasburger, H., Rentschler, I., & Jüttner, M. (2011). Peripheral vision and pattern recognition: a
1043   review. *Journal of Vision, 11*(5), 1-82.
1044 Strasburger, H., & Wade, N. J. (2015). James Jurin (1684–1750): A pioneer of crowding research?
1045   *Journal of Vision, 15*(1:9), 1-7.
1046 Tolhurst, D. J., & Ling, L. (1988). Magnification factors and the organization of the human striate
1047   cortex. *Human Neurobiology, 6*, 247–254.
1048 Tripathy, S. P., & Cavanagh, P. (2002). The extent of crowding in peripheral vision does not scale with
1049   target size. *Vision Research, 42*, 2357–2369.
1050 Van Essen, D. C., Newsome, W. T., & Maunsell, J. H. R. (1984). The visual field representation in
1051   striate cortex of the macaque monkey: Asymmetries, anisotropies, and individual variability.
1052   *Vision Research, 24*(5), 429-448.
1053 Virsu, V., & Hari, R. (1996). Cortical magnification, scale invariance and visual ecology. *Vision
1054   Research, 36*(18), 2971-2977.
1055 Virsu, V., Näsänen, R., & Osmoviita, K. (1987). Cortical magnification and peripheral vision. *Journal of
1056   the Optical Society of America A, 4*, 1568–1578.
1057 Virsu, V., & Rovamo, J. (1979). Visual resolution, contrast sensitivity and the cortical magnification
1058   factor. *Experimental Brain Research, 37*, 475-494.
1059 Watson, A. B. (1987). Estimation of local spatial scale. *Journal of the Optical Society of America A,
1060   4*(8), 1579-1582.
1061 Wertheim, T. (1894). Über die indirekte Sehschärfe. *Zeitschrift für Psycholologie & Physiologie der
1062   Sinnesorgane, 7*, 172-187.
1063 Westheimer, G. (1982). The spatial grain of the perifoveal visual field. *Vision Research, 22*, 157-162.
1064 Whitney, D., & Levi, D. M. (2011). Visual crowding: a fundamental limit on conscious perception and
1065   object recognition. *Trends in Cognitive Sciences, 15*(4), 160-168.
1066
1067